AI-67-83

INVESTIGATION OF SUPERCURRENT INSTABILITIES IN TYPE II SUPERCONDUCTORS

FINAL REPORT

CONTRACT NAS8-20552
MARSHALL SPACE FLIGHT CENTER
HUNTSVILLE, ALABAMA

ATOMICS INTERNATIONAL
A DIVISION OF NORTH AMERICAN AVIATION, INC.

AI-67-83

INVESTIGATION OF SUPERCURRENT INSTABILITIES IN TYPE II SUPERCONDUCTORS

FINAL REPORT

CONTRACT NAS8-20552
MARSHALL SPACE FLIGHT CENTER
HUNTSVILLE, ALABAMA

ATOMICS INTERNATIONAL
A DIVISION OF NORTH AMERICAN AVIATION, INC.

MAY 17, 1967

CONTENTS

FIGURES

FIGURES

I. INTRODUCTION

The study of instabilities in type II superconductors followed two parallel paths, and is reported here in two self contained sections. In the first part, the question of supercurrent capacity has been attacked experimentally. A strong correlation between current capacity and a metastable ω phase has been found. This work is a fairly direct extension of earlier work with Ti-22 a/o Nb for NASA in which various time-temperature heat treatment conditions have been used to alter the critical temperature, field, and current of the alloy.

The second section of this final report is a theoretical investigation of instabilities. It is shown that the same thermodynamic non-equilibrium situation, which gives rise to superconducting transport currents in the mixed state, and which is generally referred to as flux pinning, results in instabilities of the magnetic flux structure. A distinction has to be made between limited instabilities which are self stopping, localized events and runaway instabilities, which have a catastrophic character, disrupting the superconducting transport qualities of the specimen and which are also called flux jumps. Formulas are given to calculate the conditions for flux jumping for the simplest geometry; the influence of heat diffusion is crucial and makes accurate calculations very difficult. By contrast the criterion for stability is comparatively simple, containing only the specific heat and the temperature dependence of flux pinning. The study clearly shows how to prevent instabilities altogether by choosing materials which, over a limited temperature range, increase the flux pinning strength with increasing temperature.

II. METALLURGICAL STUDIES OF Ti-22 a/o Nb

by

D. Kramer

A. TRANSFORMATIONS IN TITANIUM-22 a/o NIOBIUM

The Ti-Nb alloy system consists of a continuous series of body-centered-cubic solid solutions at elevated temperatures known as the β phase. At lower temperatures and Nb contents, other phases are found. One of these is the equilibrium hexagonal-close-packed α phase seen in the phase diagram (Figure 1). Of more importance to the superconducting behavior in the Ti-Nb system is the metastable ω phase.

In Ti-22 a/o Nb, rapid cooling from the β phase results in its retention; if the oxygen content is low no martensite will be found. However, careful examination by transmission electron microscopy using the techniques of electron diffraction and dark field illumination reveals the presence of the ω phase. The appearance of ω in a sample rapidly cooled from 800°C is shown in Figure 2.

The ω forms coherently and homogeneously throughout the β phase with linear dimensions and spacings on the order of 50 Å. The density of the ω is conservatively estimated to be at least 10^{17} cm^{-3}. Its crystal structure is hexagonal and at this stage the composition of the ω must be the same as the parent β phase since there was no opportunity for diffusion to occur. Stiegler et al.[2] have summarized much of what is known about the ω phase in Ti and Zr binary alloys.

Subsequent annealing of the retained β matrix with ω precipitates therein may produce three changes. The density of ω precipitates may decrease, their composition may become depleted in Nb (concomittantly the β phase becomes richer in Nb) and the equilibrium α phase may form. An anneal of 1 hour in the range 350 to 450°C produces little or no change in the density of the ω precipitates. Figures 3, 4, and 5 illustrate this point. However, displacements of the J_c-H curves, seen in the following section, indicate that the β phase has become richer in Nb.

An interesting feature - not related to superconducting behavior - is the presence of dislocation loops in the samples annealed 1 hour at 400 and 450°C which may be seen in Figures 6 and 7. Such loops usually form in a metal rapidly quenched from high temperature so as to produce a supersaturation of lattice vacancies. These vacancies subsequently agglomerate and collapse leaving a dislocation loop behind.[3] In the present case, we might speculate that the excess vacancies were produced as a result of the $\beta \rightarrow \omega$ transformation. Annealing then provided them with the necessary mobility to agglomerate and form dislocation loops.

Annealing for 1 hour at 500°C produces some equilibrium α phase rendering the superconducting properties uninteresting.

Longer anneals at 350°C had little effect on size of the ω precipitates but at 400 and 450°C they have grown significantly. Figure 8 shows the ω phase in the β matrix after 72 hours at 350°C. After an anneal of 48 hours at 400°C or 24 hours at 450°C, the ω particles may be individually resolved (Figures 9 and 10). They are in the shape of an ellipsoid of revolution and their dimensions and density are given in Table 1. The major axis of the ellipsoid (hence the direction of fastest growth) is parallel to the <111> β directions.

B. CRITICAL TRANSPORT CURRENTS

At 4.2°K, critical transport currents for Ti-22 a/o Nb were measured in a transverse magnetic field with 1μv sensitivity to discriminate between zero resistance and normal behavior. Samples in the form of wires .010 to .020 in. in diameter were annealed for 3 hours at 800°C, rapidly cooled and annealed to develop the ω phase. The results are plotted as J_c-H curves and are seen in Figures 11 and 12. Samples annealed only at 800°C carried currents of the order of 10^2 A/cm^2 and are not shown.

The highest J_c at 30 kilogauss, 1×10^5 A/cm^2, was carried by a sample annealed 1 hour at 450°C (see Figure 5). Longer time anneals at 400 and 450°C yield considerably lower current densities. The curves in Figure 11 all have a maximum between 20 and 30 kilogauss which is absent in the curves of Figure 12. These, however, have an inflection point between 10 and 15 kilogauss.

TABLE 1

SIZE AND DENSITY OF ELLIPSOIDAL ω PRECIPITATES
AFTER SEVERAL THERMAL TREATMENTS IN Ti-22 a/o Nb SAMPLES

Treatment	Major Axis (Å)	Minor Axes (Å)	Density (cm^{-3})	Spacing (cm)	Field for Equivalent Fluxoid Spacing (kilogauss)
Cooled from 800°C	on the order of 50		$> 10^{17}$	$< 2 \times 10^{-6}$	30
48 hours at 400°C	520	95	10^{16}	5×10^{-6}	10
24 hours at 450°C	1100	500	10^{15}	1×10^{-5}	5

The shapes of the curves may be qualitatively understood in terms of flux pinning. The ability of a type II superconductor to sustain a zero-resistance transport current in an external magnetic field is due to the presence of microstructural features which impede the motion of penetrating magnetic flux and are referred to as pinning sites. The pinning strength is the reaction of the bulk superconductor to the Lorentz forces which the magnetic flux is subjected to in the presence of transport currents.

The critical transport current is reached when the Lorentz force becomes greater than the pinning strength. This allows the flux to move through the superconductor resulting in a small voltage drop. At low fields (< 5 kilogauss), much of the current is at the surface of the specimen and does not reflect bulk properties.

Magnetic flux inside the superconductor is quantized in individual flux lines which contain a quantum

$$\phi_o = 2.07 \times 10^{-7} \text{ gauss-cm}^{-2}$$

The spacing of these flux lines is given by

$$d = \left(\frac{\phi_o}{B}\right)^{\frac{1}{2}}$$

Maximum pinning strength occurs when there is one flux line to each pinning site. These sites provide local energy minima for fluxoids (quantized flux lines) and are effective traps for only one fluxoid. More than one per site reduces the pinning strength as does the opposite case which leaves pinning sites empty. The details of flux pinning are complicated by mutual interaction of fluxoids, their local distortion and the field and temperature dependence of pinning strength.[4]

C. CORRELATION OF MICROSTRUCTURE WITH J_c-H CURVES

In Ti-22 a/o Nb, the pinning sites are the ω phase precipitates. Although the density of pinning sites is the same for all the curves in Figure 11, they are displaced vertically because the composition of the ω and β phases changes during annealing after the 800°C treatment. The ω phase becomes richer in Ti

and the β phase in Nb. This raises the upper critical field of the β phase[5] and the pinning strength due to the greater composition difference between the phases. After longer anneals (Figure 12), the pinning strength declines due to a reduction in ω precipitate density even though each individual precipitate may trap fluxoids more effectively.

The maxima in the J_c-H curves of Figure 11 are associated with maximum pinning. The last column in Table 1 is the calculated value of the field H from Equations 1 and 2 to give a fluxoid spacing equal to the precipitate spacing. At these fields, B and H are nearly identical. For the samples of Figure 11, the maximum in the J_c-H curve does occur near the 30 kilogauss calculated.

For the curves of Figure 12 from samples with coarser precipitate structures, maxima are probably masked out by other effects. However, inflections in the curves do occur near the field calculated in Table 1. A similar analysis has been given by Sutton and Baker[6] for the case of Ti-32 w/o Nb.

Although a sample annealed 48 hours at 400°C has a higher density of pinning sites than one annealed 24 hours at 450°C, the latter has a higher J_c. This is probably owing to a greater Nb content in the matrix and more effective pinning per site.

ACKNOWLEDGMENTS

The electron microscopy was performed by Cecil G. Rhodes at the North American Aviation Science Center. Derald R. Warner assisted with the superconductivity measurements.

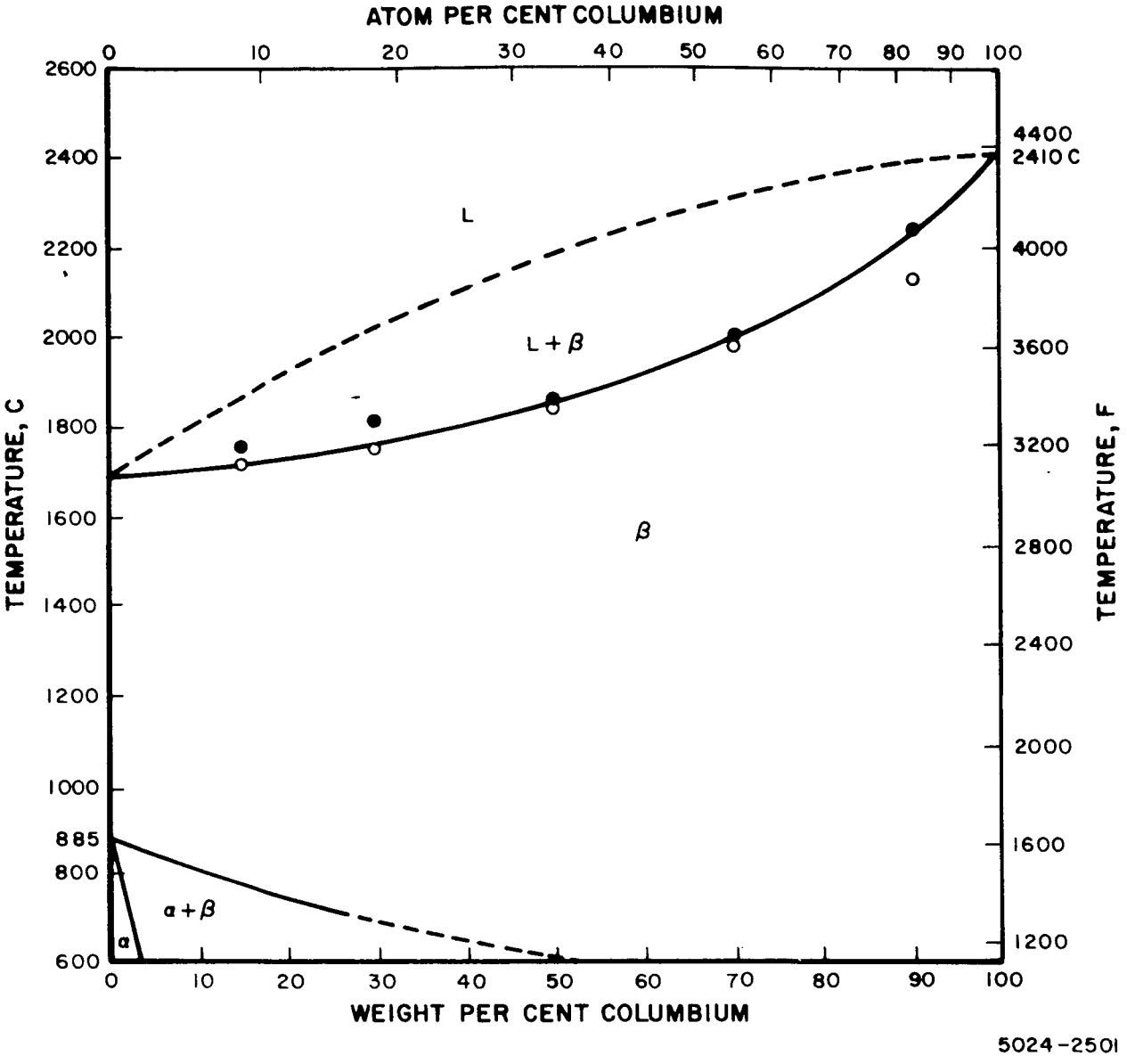

Figure 1. The Ti-Nb Phase Diagram

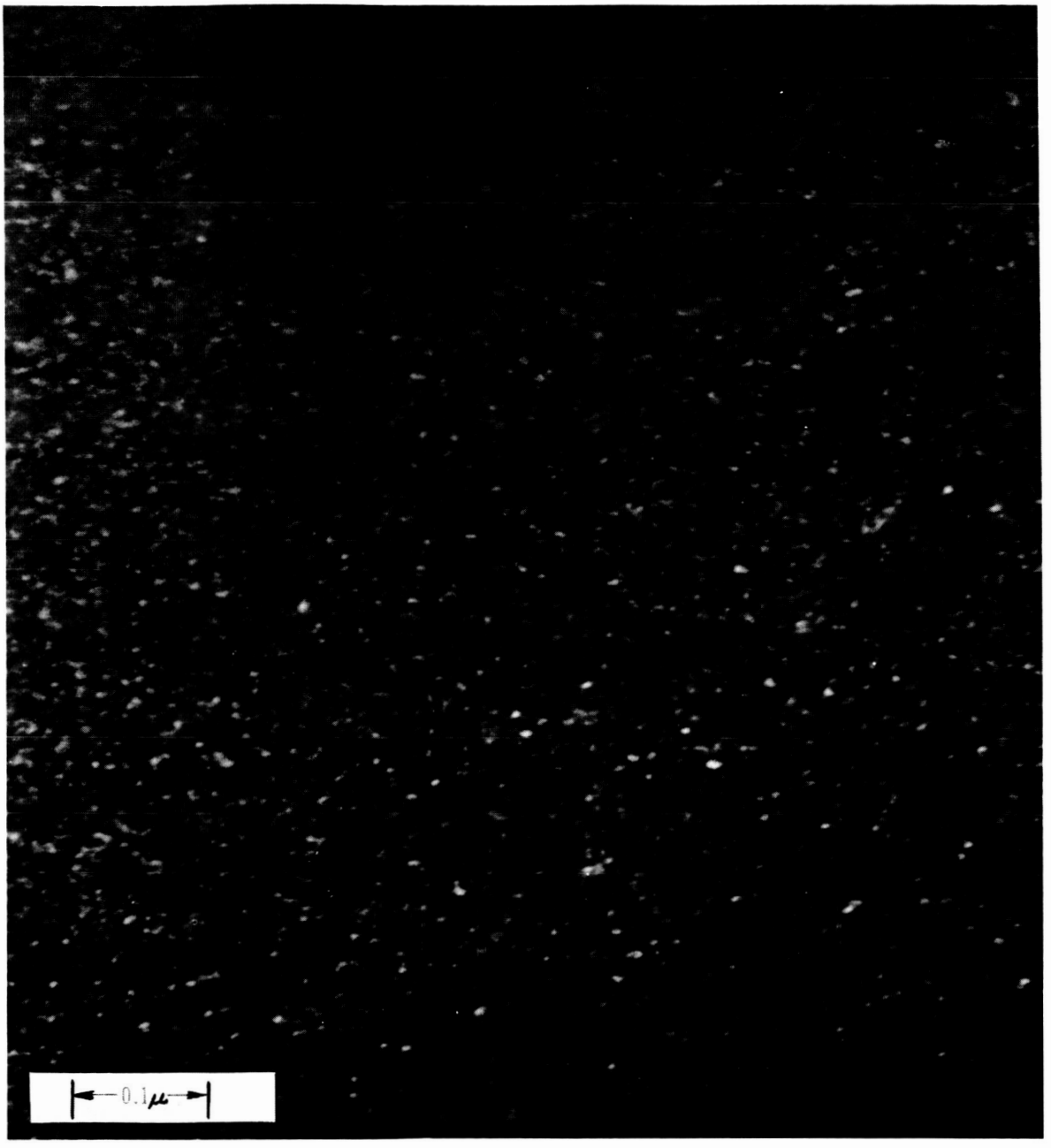

Figure 2. Transmission Electron Photomicrograph of Ti-22 a/o Nb Rapidly Cooled from 800°C (β Phase)

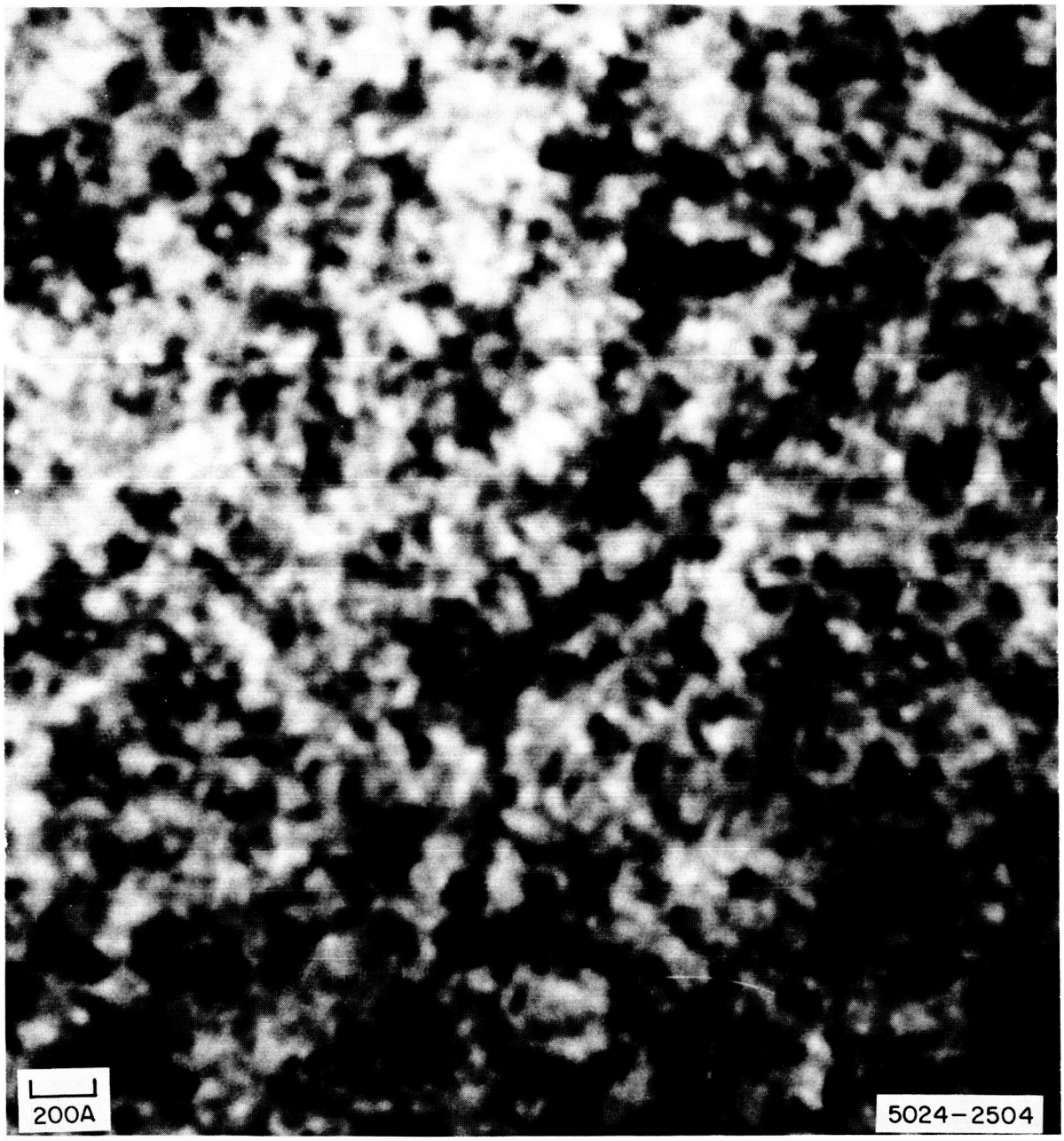

Figure 3. Transmission Electron Photomicrograph of Ti-22 a/o Nb Rapidly Cooled from 800°C and Annealed 1 Hour at 350°C

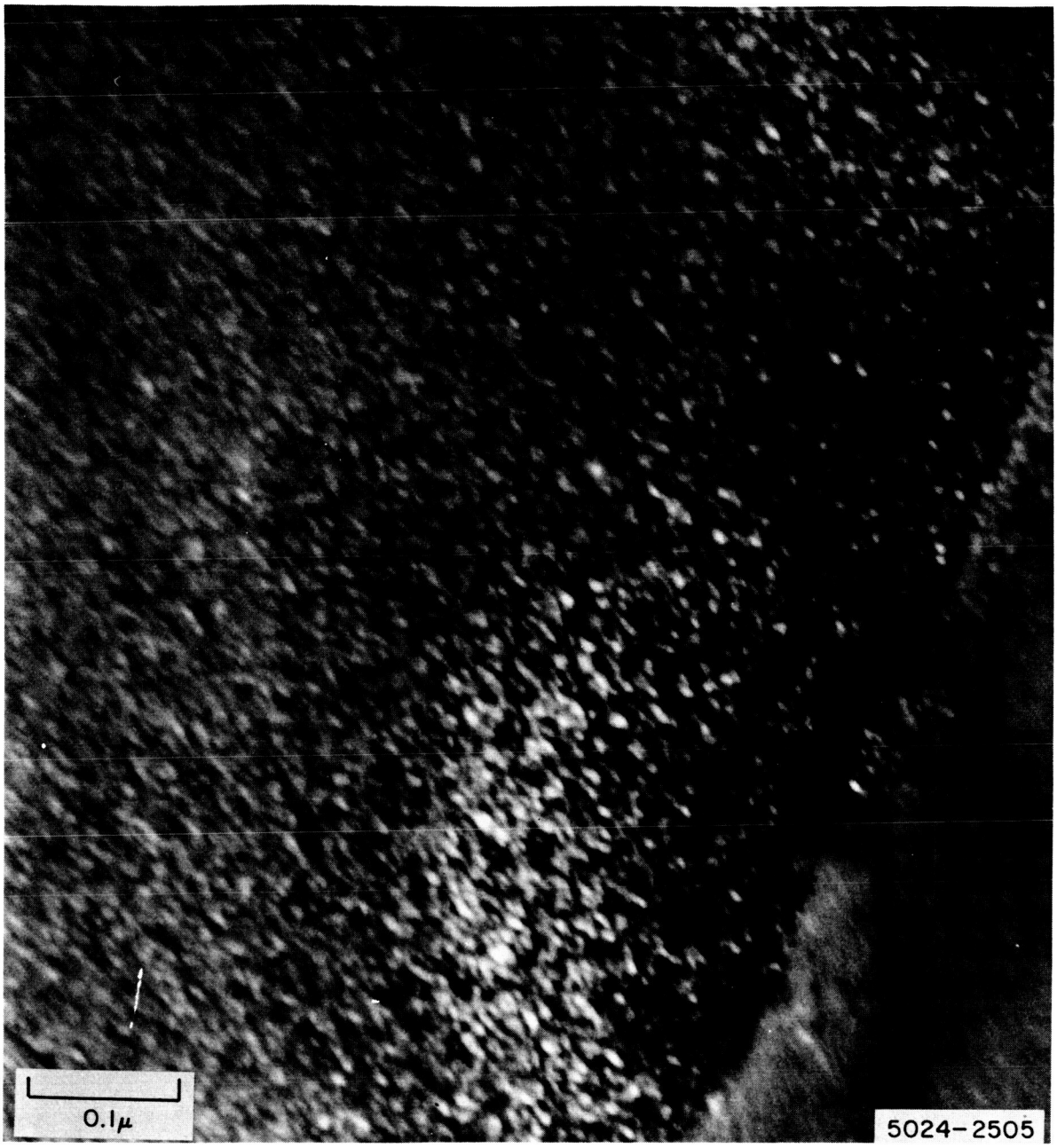

Figure 4. Transmission Electron Photomicrograph of Ti-22 a/o Nb Rapidly Cooled from 800°C and Annealed 1 Hour at 400°C

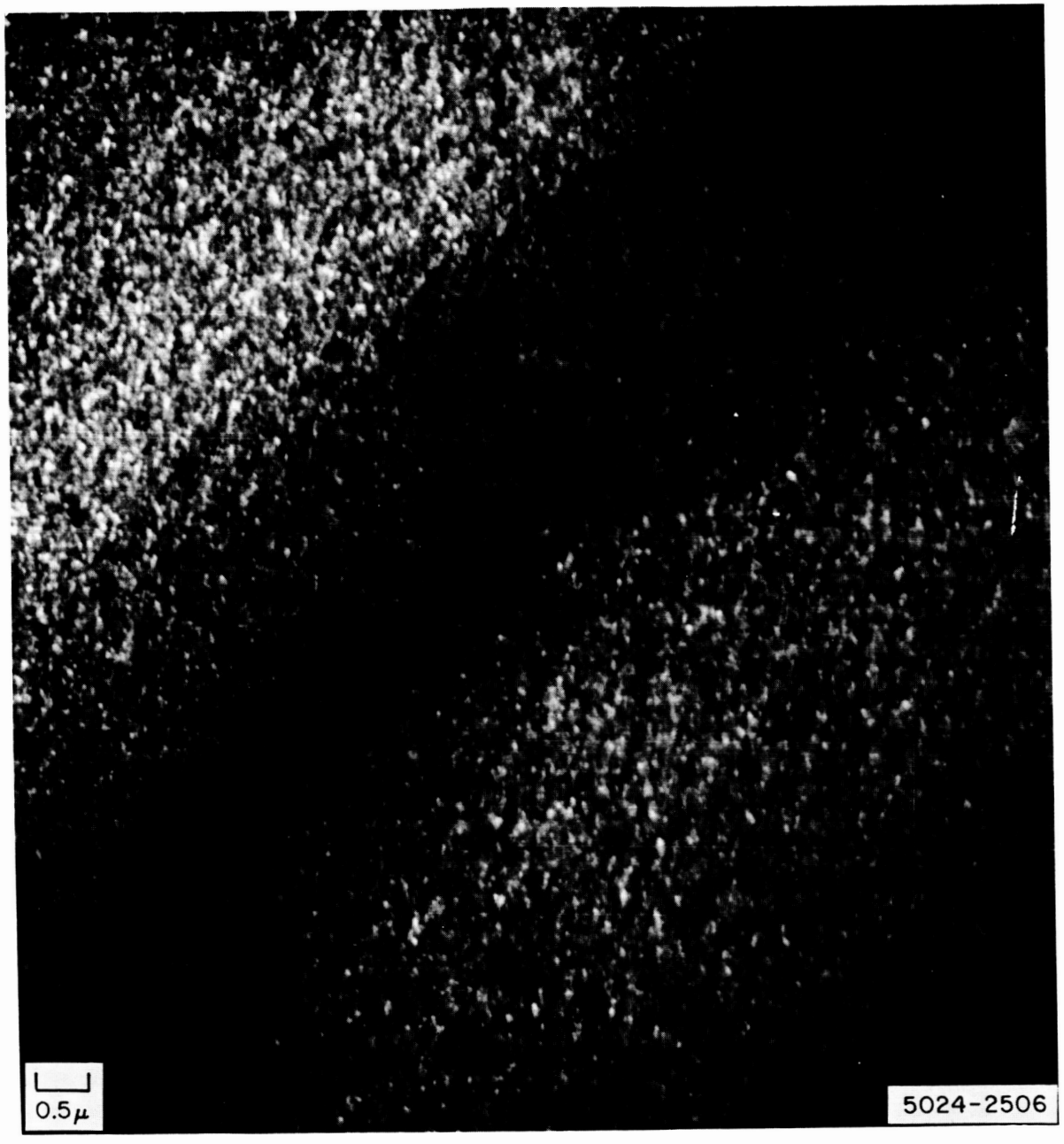

Figure 5. Transmission Electron Photomicrograph of Ti-22 a/o Nb Rapidly Cooled from 800°C and Annealed 1 Hour at 450°C

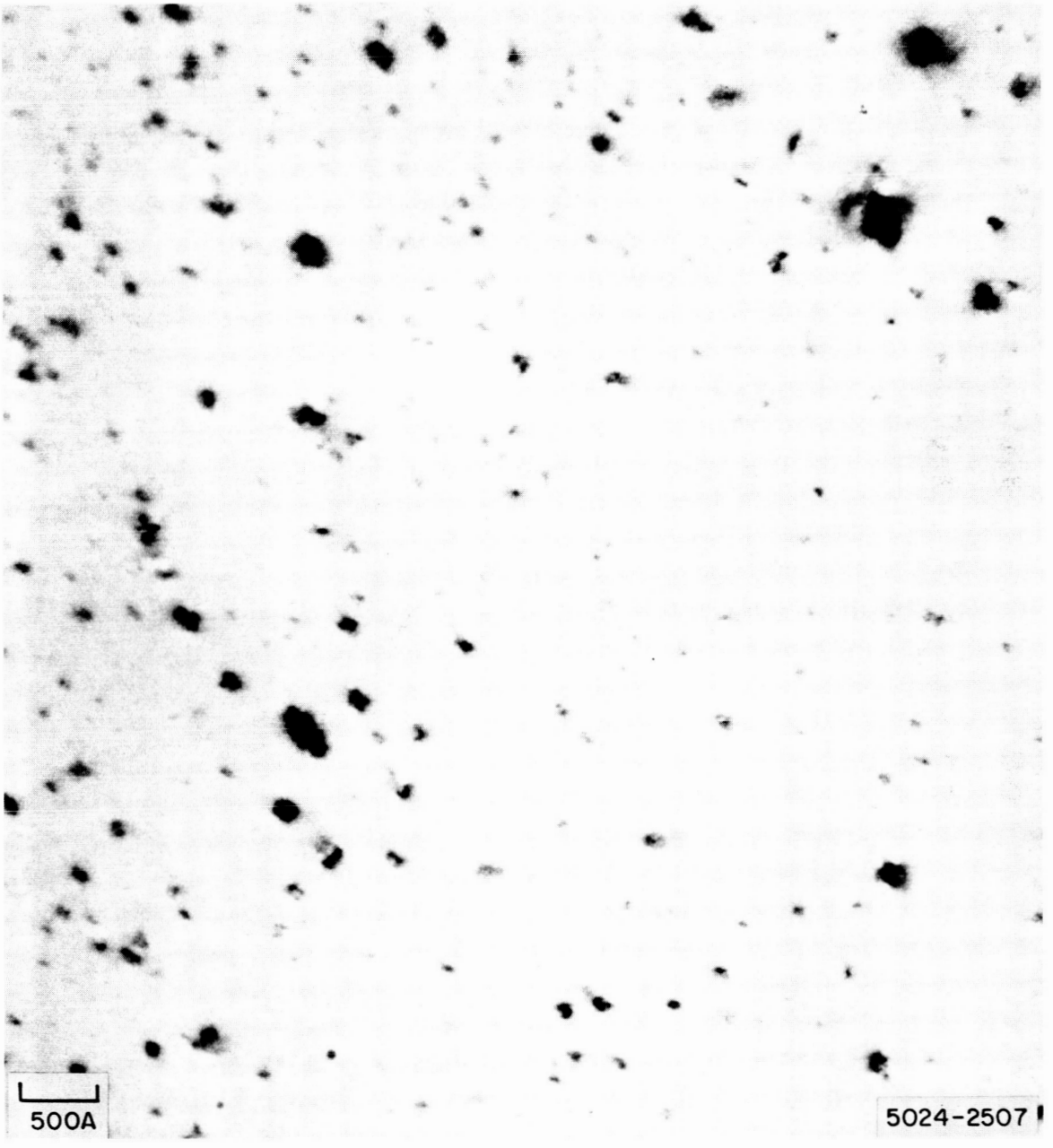

Figure 6. Transmission Electron Photomicrograph of Ti-22 a/o Nb Rapidly Cooled from 800°C and Annealed 1 Hour at 400°C. Dislocation Loops Are Seen.

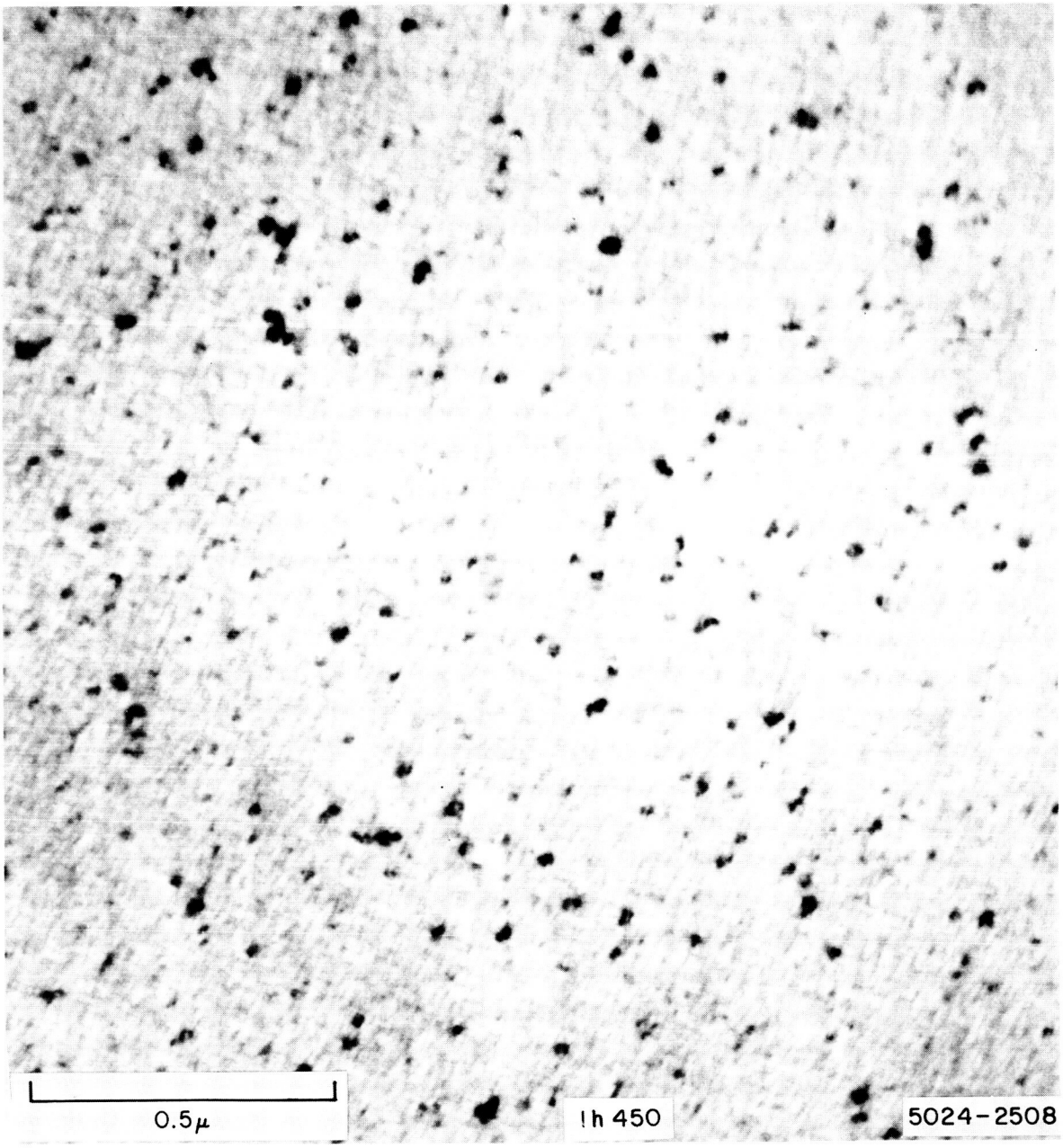

Figure 7. Transmission Electron Photomicrograph of Ti-22 a/o Nb Rapidly Cooled from 800°C and Annealed 1 Hour at 450°C. Dislocation Loops Are Seen.

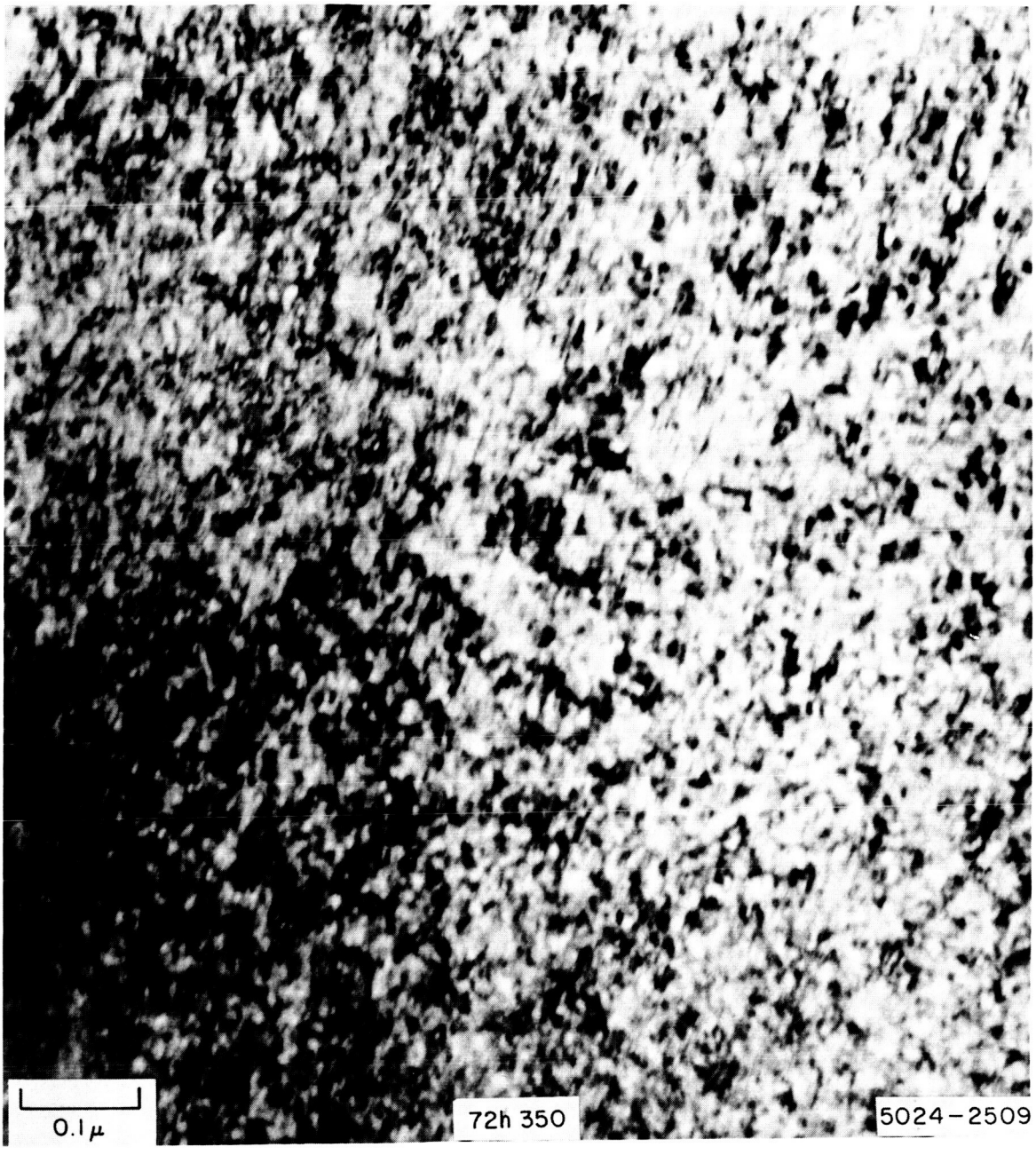

Figure 8. Transmission Electron Photomicrograph of Ti-22 a/o Nb Rapidly Cooled from 800°C and Annealed 72 Hours at 350°C

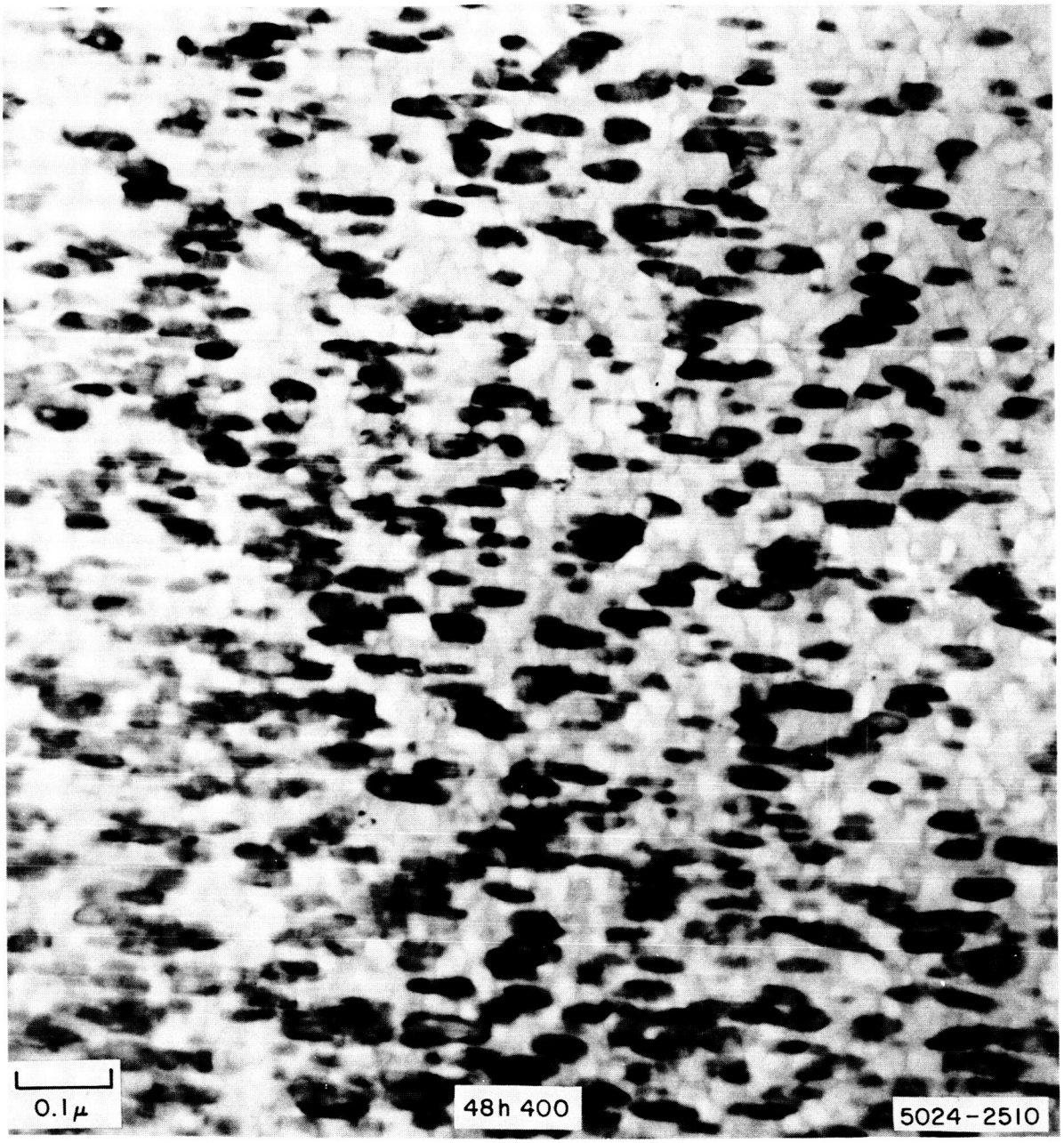

Figure 9. Transmission Electron Photomicrograph of Ti-22 a/o Nb Rapidly Cooled from 800°C and Annealed 48 Hours at 400°C

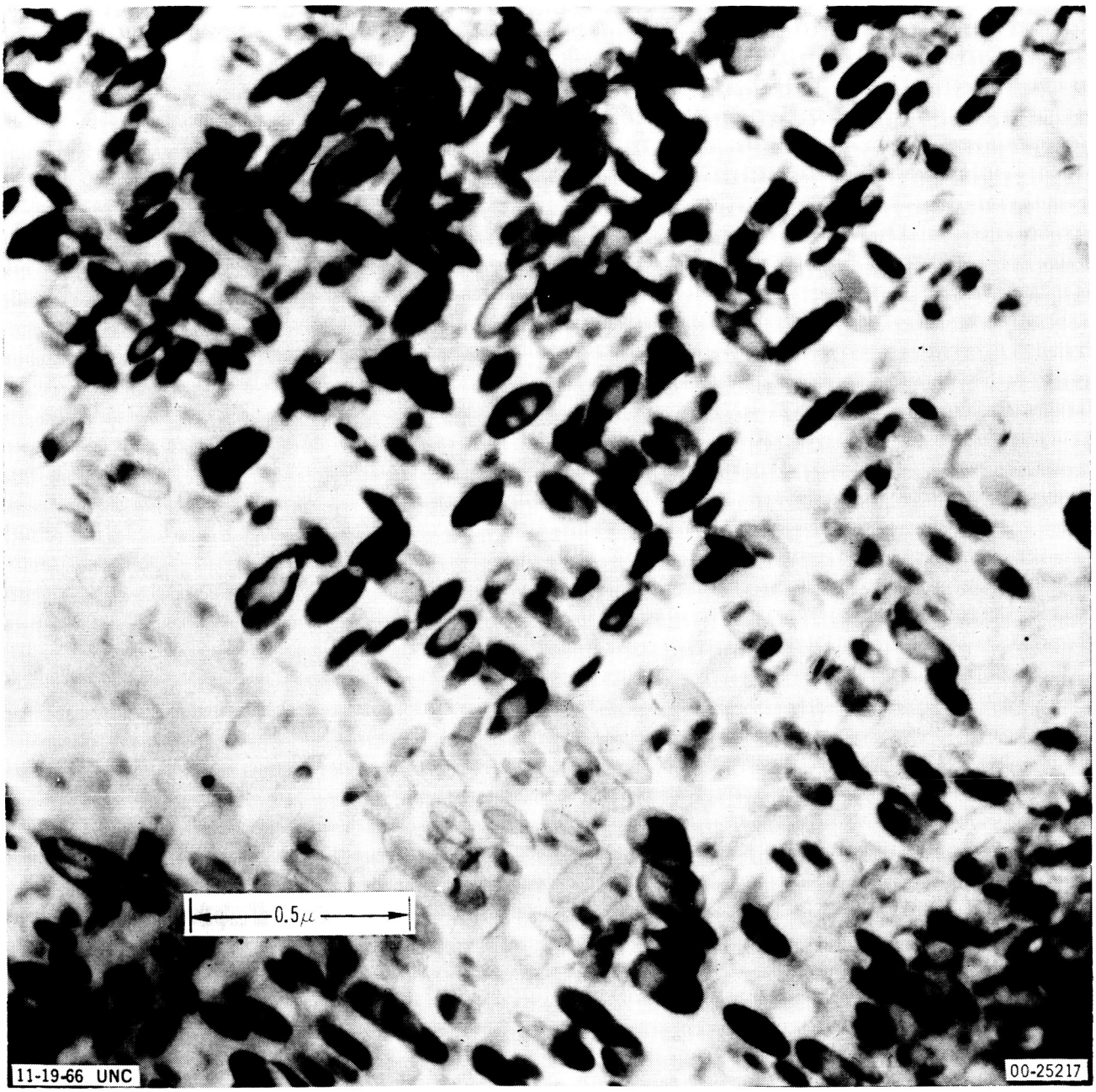

Figure 10. Transmission Electron Photomicrograph of Ti-22 a/o Nb Rapidly Cooled from 800°C and Annealed 24 Hours at 450°C

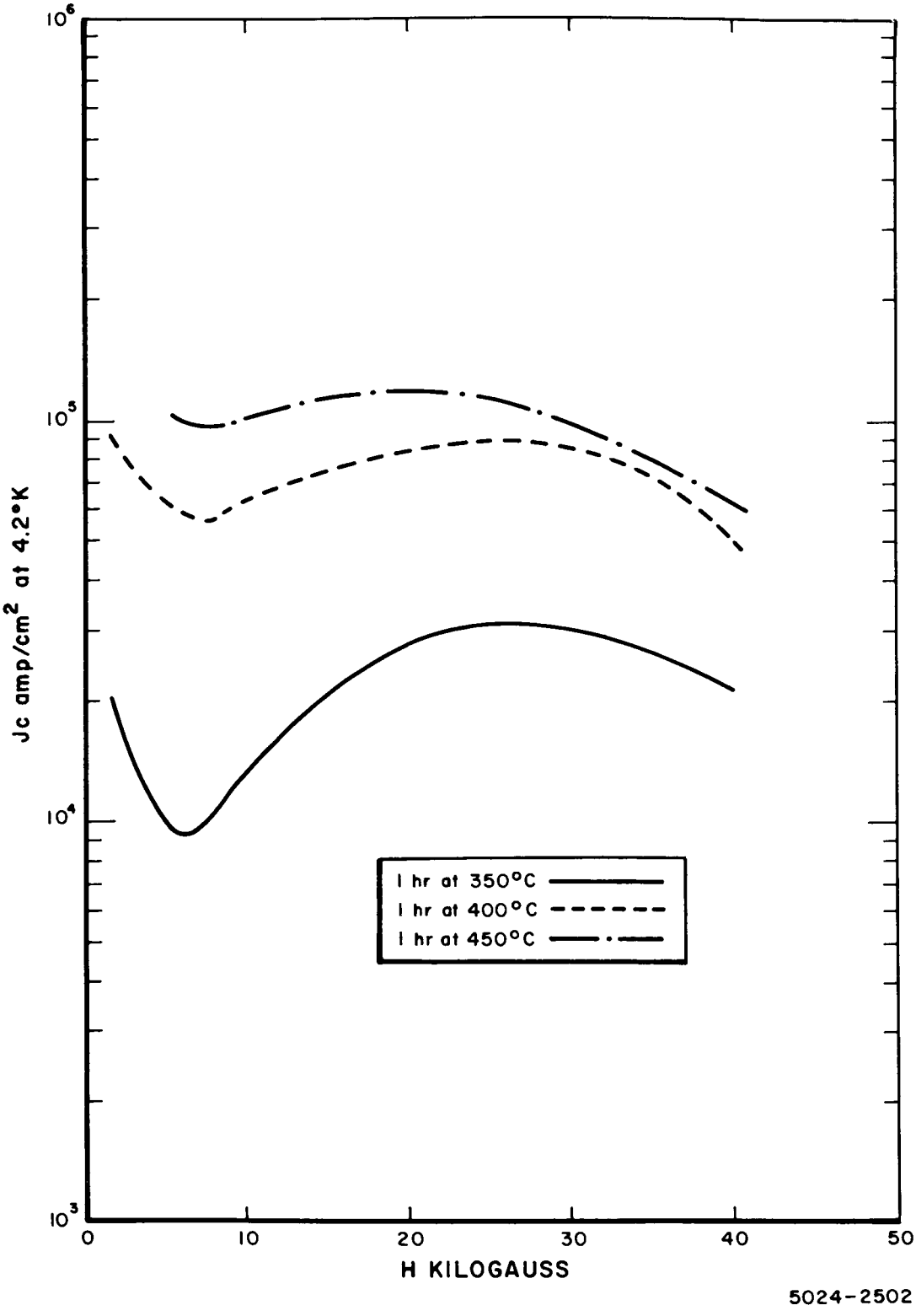

Figure 11. Critical Current Density, J_c, vs Transverse External Field, H, at 4.2°K for Ti-22 a/o Nb Samples Rapidly Cooled from 800°C and Annealed as Indicated

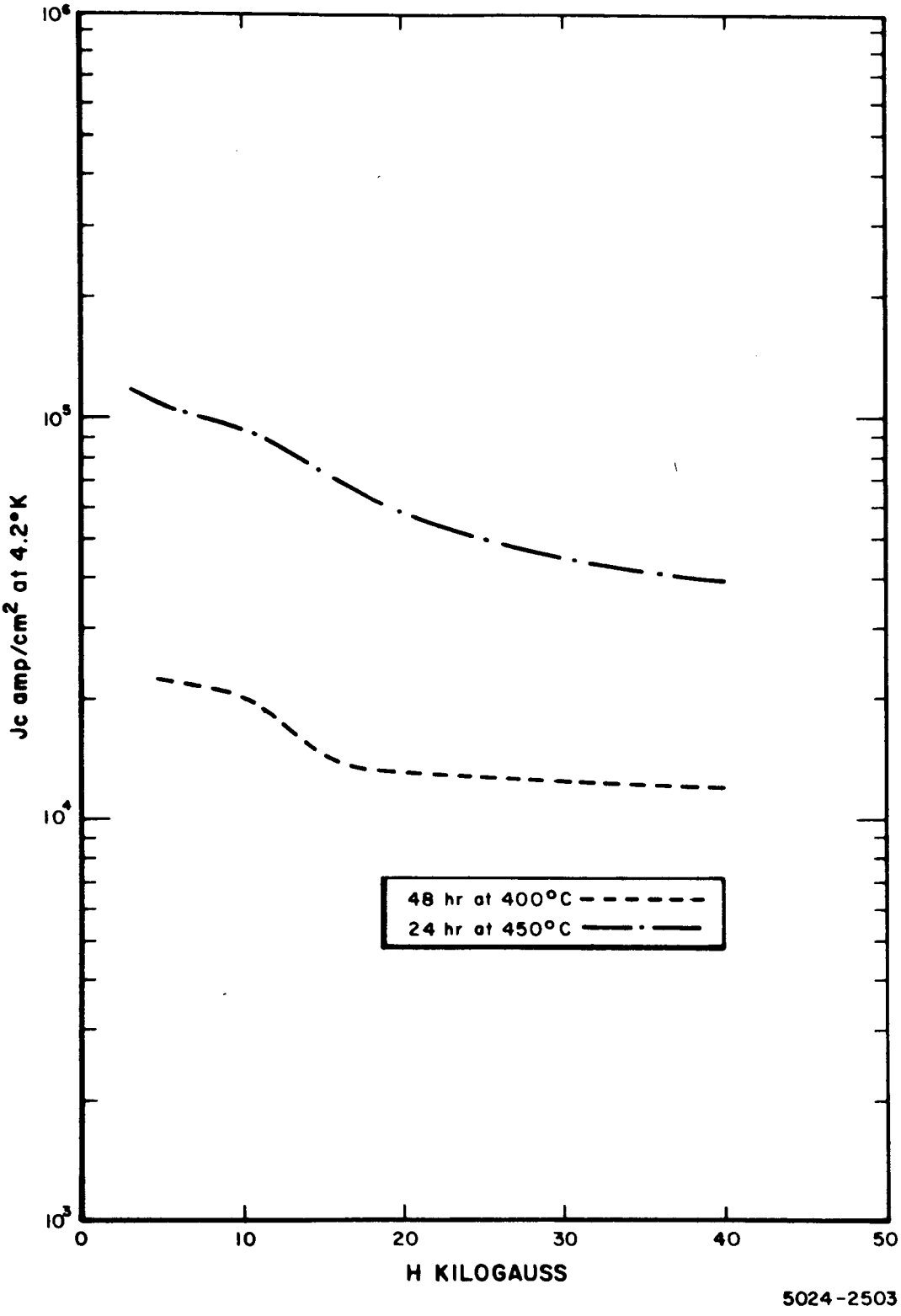

Figure 12. Critical Current Density, J_c, vs Transverse External Field, H, at 4.2°K for Ti-22 a/o Nb Samples Rapidly Cooled from 800°C and Annealed as Indicated

III. STABILITY STUDIES FOR TYPE II SUPERCONDUCTORS

by

S. L. Wipf

A. STABILITY REVIEW

Flux jumps[7-9] and critical current degradation in coils[10] have been variously observed in all technically important high field superconductors. Both are manifestations of the very general phenomenon of magnetic instabilities in type II superconductors.

Inconsistency and scattering of experimental results at first gave support to the idea that gross material imperfections and weak spots are responsible for these effects. But this interpretation has been ruled out except for a few isolated cases as more experimental evidence has been accumulated.

There has been no lack of qualitative discussions[7,11-14] but attempts at quantitative explanations have been hampered by the complexity of the problem and the scarcity of data for important parameters such as specific heat, thermal conductivity or diffusivity, resistance in the critical state, etc.

The present investigation outlines a quantitative treatment of magnetic instabilities for the very simple experimental situation of a sufficiently thick, long, solid cylinder (without transport current) in a parallel external field which is changing at a constant rate. In this case, the assumption of a plane semi-infinite superconductor in a parallel field allows a somewhat simpler calculation while being a good approximation. The aim is to find the value of the external field for which a flux jump takes place.

It may help to summarize briefly the experimental facts in order to illustrate what is understood by a flux jump. If the external field, H, is raised from zero, the field, B, inside the solid cylinder will stay zero except in a layer adjacent to the surface in which shielding currents (parallel to surface and at right angle to the field direction) are induced.[15-18] This "shielding layer" will grow in thickness as H increases until, above a certain value of H, the shielding currents suddenly break down and B throughout the

cylinder becomes practically equal to H. On further increase of H, the process will repeat itself; a shielding layer growing to a certain thickness before breaking down again and so on. The break-down process is generally called flux jump.

B. BASIC APPROACH

Preceding the detailed mathematical procedure, an outline of the physical ideas is helpful. We visualize the mixed state in terms of quantized flux lines or fluxoids inside the superconductor whose density, n, gives the induction $B = n \varphi_o$, (flux quantum $\varphi_o = 2.07 \times 10^{-7}$ gauss cm^2). The current density, j, in the shielding region is connected through the Maxwell equation, curl $B = 4\pi j$, with the gradient of the induction

$$\frac{1}{4\pi} \frac{\partial B}{\partial x} = - j \qquad \ldots(1)$$

(The x axis is normal to the surface with the positive direction into the superconductor; see Figure 13.)

In the presence of this current density, a Lorentz force, F_L, is acting on the flux structure

$$F_L = B \times j = - \frac{B}{4\pi} \cdot \frac{\partial B}{\partial x} \qquad \ldots(2)$$

The reaction to this force is provided by inhomogeneities in the material creating local variations of the mean free energy of the flux structure.[19] If a force equal to the local energy gradient is applied, a fluxoid will leave its minimum energy site and move into the neighboring minimum after the energy maximum in between has been passed. The energy between maximum and minimum is completely dissipated. This concept is called flux pinning and the imperfections responsible for it are vaguely referred to as pinning sites. These can be thought of as extended defects creating a network of energy maxima or as point defects of energy minima. Suggested examples are dislocations[20] and grain boundaries for the former, cavities[21] and impurities, for the latter. But for the present argument, the details of flux pinning are of no concern. One may simply assume a uniform distribution of volume density ρ of pinning sites, each of strength P, resulting in a total pinning force per unit volume

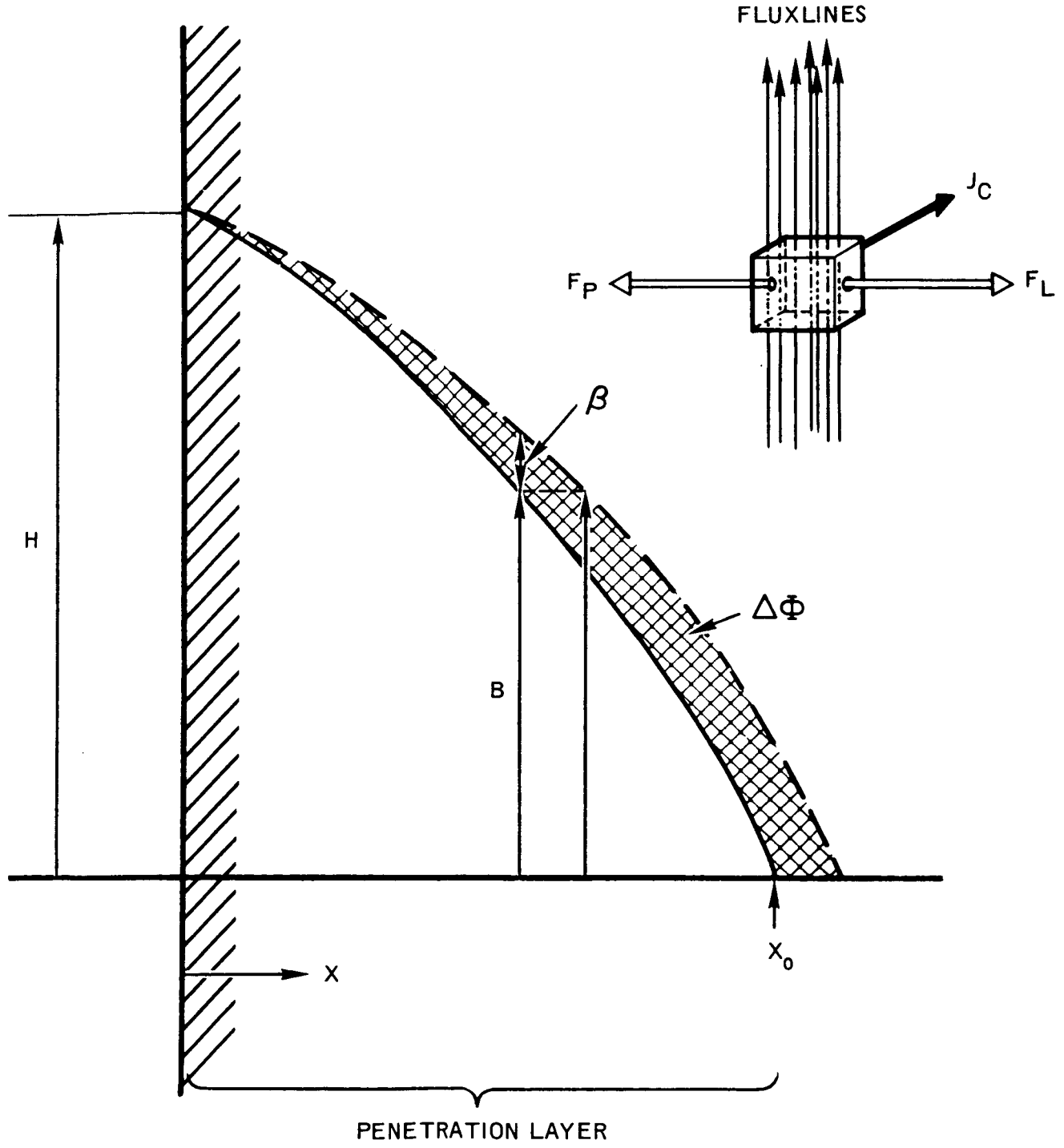

Figure 13. Illustration of Penetration Layer and Disturbance, and of Flux Structure in Equilibrium Between Lorentz and Pinning Forces

of $F_P = \rho P$. F_P is a function of B and temperature T.[4]

A second contribution to the Lorentz force reaction, independent of flux pinning, comes from the flux flow resistance[22] which is characterized by a viscosity η. If the actual speed of the flux lines is v, this contribution becomes ηv. Dissipative mechanisms in flux flow have been discussed extensively.[23-26]

It is found* that for low temperatures and fields, experimental results can be expressed as $\eta = c_\eta B$ where $c_\eta = H_{c2}/\rho_n$ with H_{c2} the upper critical field at zero temperature and ρ_n the normal state resistivity. c_η is constant over a large range of temperature and field.

Therefore, in the shielding layer in equilibrium, the Lorentz force is balanced by pinning and viscous forces.

$$F_L = F_P + \eta v \qquad \ldots(3)$$

The task will be to discuss the stability of this equation against disturbances.

Let us first introduce and justify two approximations. When v is very small (at the onset of an instability), one may neglect the viscous term. This is equivalent to assuming isothermal conditions throughout the specimen, for then j becomes a function of B only and in order to match B and H at the surface the fluxoids have to have a drift velocity

$$v_{dr} = \frac{dH}{dt} \Big/ \frac{\partial B}{\partial x} \quad (x = o) = \frac{dH}{dt} \Big/ 4\pi j \quad (B = H) \qquad \ldots(4)$$

The power dissipation becomes

$$j \cdot \frac{d\Phi}{dt} = j \cdot n \cdot \varphi_o \cdot v_{dr} = \frac{dH}{dt} \cdot \frac{B}{4\pi} \qquad \ldots(5)$$

which enables one to estimate the limits of the isothermal approximation.**

---

* In Reference 22 Equation (15), there is (per unit flux line): $\eta_{emp} = \varphi_o H_{c2}(o)/\rho_n c^2$, in order to express a volume force here $\eta = n\,\eta_{emp}$.

** If we consider typical order of magnitude values: $j > 10^4$ A/cm^2, $H < 10^4$ G, $dH/dt < 10^4$ G/sec, we have $v < 1$ cm/sec, power dissipation < 1 W/cm^3 resulting in a power transfer of < 0.5 W/cm^2 across the surface into the helium since the shielding layer will be < 1 cm thick. This power transfer is below the film boiling limit (~ 0.8 W/cm^2)[22] which would thermally isolate the surface from the bath.

A disturbance of this equilibrium takes the character of an addition of a flux increment, $\Delta\Phi$, to the interior of the body. This may be thought of as occurring when the innermost flux line moves a small distance, see Figure 13. Such a disturbance can be imagined as a density wave in the fluxoid structure which propagates orders of magnitude* faster than the drift velocity. This justifies the assumption of a constant H during the time of a disturbance.

So, using these two approximations, $v = o$ simplifies the equilibrium Equation (3) to

$$F_L = F_P \qquad \ldots(6)$$

and H = constant causes the flux front to take on the shape indicated in Figure 13 after a disturbance.

The disturbance changes both Lorentz and pinning force. From Figure 13 one sees immediately that on the whole the Lorentz force has been reduced since for a point with the same B the gradient has become smaller. The pinning force has also changed because of the change in temperature due to the energy dissipated by adding $\Delta\Phi$. The dissipation can be represented by the product of the induced voltage and the shielding current density or, with the same result, by the movement of flux lines against the pinning forces. The change of the pinning force is also negative when, as in most superconductors, increasing temperature reduces pinning strength. If the reduction of the Lorentz force is larger than the reduction of the pinning force, the equilibrium is stable; if smaller then it is unstable; equality gives the stability limit.

A qualitative conclusion may illustrate the point. In Figure 14a are shown two shielding layers with equal $\Delta\Phi$ disturbances, $\Delta\Phi$ being represented by the shaded area. When H is small, the reduction of the Lorentz force is greater than when H is large. The reduction in pinning strength is similar in both cases since it depends mainly on $\Delta\Phi$. This means that the stability limit is approached with increasing H. Looking now at a limited superconductor such as a plane slab or a cylinder in Figure 14b, it is found that after the field has penetrated to the center, a disturbance with the same reduction in Lorentz

* A measurement of the magnetic diffusivity[28] in NbZr gave a factor of 10^3.

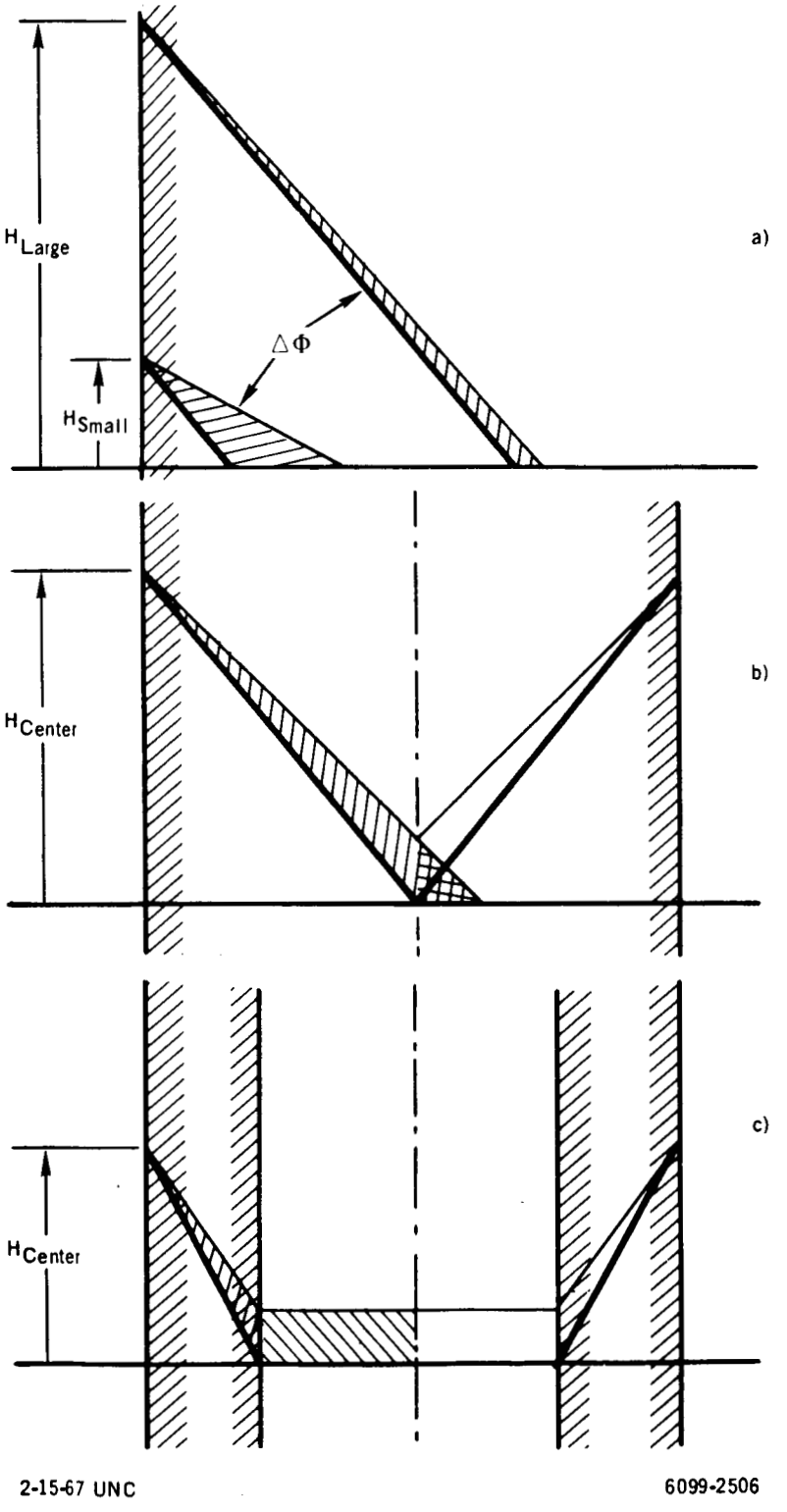

Figure 14. Influence of the External Field on the Disturbance. Dependence on Sample Geometry for a Solid and a Hollow Cylinder.

force needs an amount of $\Delta\Phi$ slightly smaller than before by the cross hatched area since flux comes in from both sides. This lends plausibility to the frequent observation that if the center of a specimen is reached by the field without a flux jump taking place, the danger of flux jumping is reduced. If on the other hand the specimen is a hollow cylinder as in Figure 14c, then the flux jumping danger is increased suddenly, as soon as the field reaches the inside wall, because an increase in $\Delta\Phi$ is now needed to fill the hole.

On exceeding the stability limit, the Lorentz force becomes greater than the pinning force during a disturbance and the movement of the flux lines will accelerate. Now one has to look at Equation (3) since v can be neglected no longer. With the acceleration of the flux lines, the disturbance grows larger and may develop into a flux jump. The acceleration process will take some time during which thermal conduction reduces the temperature rise and therefore, to a certain extent, restores the pinning strength of the material. This will reduce the acceleration and eventually decelerate the flux lines again. The result will be a large, but locally and in time limited, disturbance as distinct from a flux jump, described in the introduction. This situation may be termed as one of limited instability.

Limited instability is characterized by an acceleration to a maximum speed of the flux lines followed by deceleration. The duration of this process is short enough that the shielding layer has not grown noticeably compared to the original thickness x_o. If, however, $\int v dt$ becomes comparable to x_o during the acceleration process, then the heat conduction, both to the surface of the specimen and across the inner boundary of the shielding layer, which should reduce the temperature and thus restore the pinning, becomes less effective. Eventually the shielding layer may grow so rapidly that the heat conduction becomes negligible, i.e., the front of the advancing flux may outrun the heat conduction, resulting in an adiabatic process. This runaway instability then is a flux jump.

A graphic representation summarizing the basic approach is given in Figure 15.

The following three sections will give a quantitative treatment along the given outline for the regions of full stability, limited instability, and runaway instability.

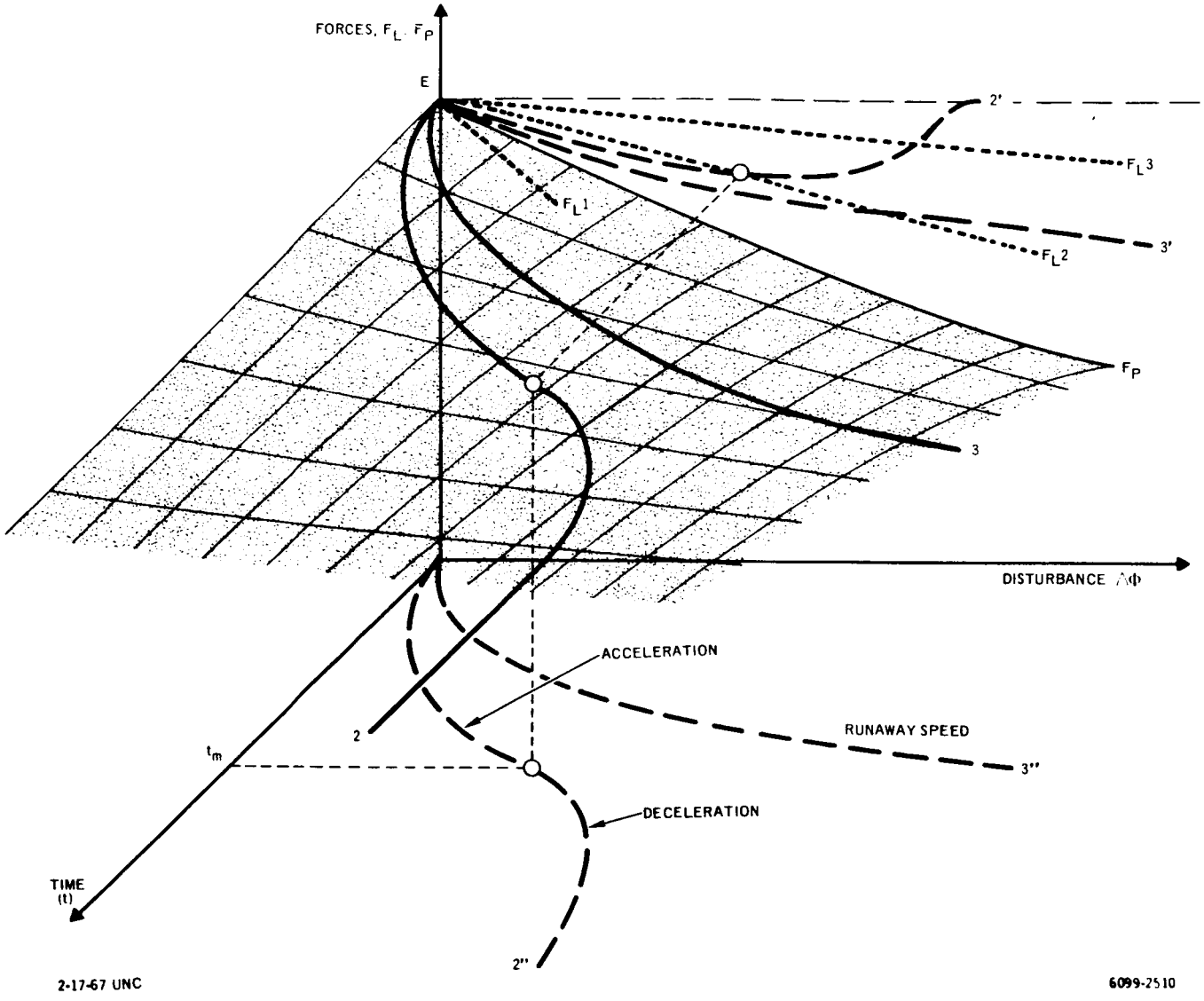

Figure 15. Graphic Representation of Basic Approach. Equilibrium is represented by point E where $F_L = F_P$. It is shown how F_P might be affected by an increasing disturbance $\Delta\Phi$. If the Lorentz force changes as indicated by F_L 1 then the equilibrium is stable. The limit of the stability region is found when F_L and F_P have the same tangent at E. A limited instability is illustrated by F_L 2; this causes F_P to change as curve 2 lying on the surface which indicates how F_P recovers with time due to heat conduction. The projection 2' gives the point of maximum speed where it crosses F_L 2, it is the inflection point on the projection 2" into the t, $\Delta\Phi$ plane. F_L 3 indicates a runaway instability. The runaway speed is reached when 3' becomes parallel to F_L 3. A linear approximation of F_L is assumed.

C. FULL STABILITY

A disturbance of the shielding layer can be introduced by changing B(x) into B(x) + β(x) where β(x) is an infinitesimally small positive field. This will change Lorentz and pinning force from F_L into $F_L + \Delta F_L$ and F_P into $F_P + \Delta F_P$. The equilibrium Equation (6) changes into

$$F_L + \Delta F_L \begin{matrix} \text{instability} \\ \geqq \\ < \\ \text{stability} \end{matrix} F_P + \Delta F_P \qquad \ldots(7)$$

The equal sign, belonging either to instability or to stability, separates the two regions and determines what we call the stability limit. We want to solve

$$\Delta F_L = \Delta F_P \qquad \ldots(8)$$

Since, as said before, a disturbance spreads out very quickly, we can ask that (8) be fulfilled simultaneously for all x.*

One gets using Equation (2)

$$\Delta F_L = F_L (B + \beta) - F_L (B) = -\frac{1}{4\pi} \left(B \frac{d\beta}{dx} + \beta \frac{\partial B}{\partial x} \right) \qquad \ldots(9)$$

$\beta d\beta/dx$, being small to the second order, can be neglected.

The pinning strength is mainly affected by the temperature rise which accompanies the energy dissipation due to the admission of flux, and to a much smaller extent by the increase in field. Thus $\Delta F_P = (\partial F_P/\partial T)\, \Delta T + (\partial F_P/\partial B)\, \beta$.

The energy dissipated is

$$\Delta q = j \cdot \Delta \varphi = -\frac{1}{4\pi} \frac{\partial B}{\partial x} \int_x^{x_o} \vartheta dx \qquad \ldots(10)$$

* It can be shown that if $\Delta F_L > \Delta F_P$ for $x_1 < x < x_2$ and $<$ for $x < x_1$, $x > x_2$ then the flux lines in $x_1 < x < x_2$ will accelerate in such a way as to reduce the differences between ΔF_L and ΔF_P in both intervals.

The initial temperature rise becomes

$$\Delta T = \frac{1}{c} \Delta q \qquad \ldots(11)$$

where c is the specific heat per unit volume. Here we have again made use of the fact that the disturbance is a quick process compared to dH/dt and avoid using the exact (but cumbersome) heat equation

$$\frac{\partial T}{\partial t} = \alpha_{th} \frac{\partial^2 T}{\partial x^2} + \frac{1}{c} \frac{dq}{dt} \qquad \ldots(12)$$

with α_{th} being the thermal diffusivity, for which (11) is a solution for small enough t. (See Sections D and E.)

With (10) and (11) we have now

$$\Delta F_P = - \frac{\partial F_P}{\partial T} \cdot \frac{1}{4\pi c} \cdot \frac{\partial B}{\partial x} \int_x^{x_o} \beta dx + \frac{\partial F_P}{\partial B} \cdot \beta \qquad \ldots(13)$$

Equating (9) and (13) one gets

$$B \cdot \frac{d\beta}{dx} + \left(\frac{\partial B}{\partial x} + 4\pi \frac{\partial F_P}{\partial B} \right) \beta - \frac{1}{c} \frac{\partial B}{\partial x} \cdot \frac{\partial F_P}{\partial T} \int_x^{x_o} \beta dx = 0 \qquad \ldots(14)$$

Now we have to find the field H for which (14) has a solution with the following boundary conditions

$$1.\ \beta(0) = 0 \qquad \text{and} \qquad 2.\ \beta(x_o) = D\ (= \text{const.}) \qquad \ldots(15)$$

This field will give the stability limit and may be denoted as H_{fi}.

H_{fi} can only be calculated if $F_P(B,T)$ is known.

In what follows we shall determine H_{fi} for a dependency of F_P which is found to be a good empirical approximation in many cases.[29]

$$F_P = \alpha \cdot \frac{B}{B + B_o} \qquad \ldots(16)$$

and

$$\frac{\partial F_P}{\partial T} = \frac{\partial \alpha}{\partial T} \frac{B}{B + B_o} \qquad \ldots(17)$$

where

$$\frac{\partial \alpha}{\partial B} = \frac{\partial B_o}{\partial T} = 0$$

Using (6) and (2) in (16), one finds the differential equation

$$\frac{\alpha}{B + B_o} + \frac{1}{4\pi} \frac{\partial B}{\partial x} = 0 \qquad \ldots(18)$$

With the boundary condition for $x = 0$, $B = H$ the solution becomes

$$(H + B_o)^2 - (B + B_o)^2 = 8\pi\alpha x \qquad \ldots(19)$$

or

$$\left[(H + B_o)^2 - 8\pi\alpha x\right]^{\frac{1}{2}} - B_o = B \qquad \ldots(19')$$

Substituting (17) - (19) into (14), differentiating and using the notation $S = \frac{1}{c} \frac{\partial \alpha}{\partial T}$ and $R = (B_o + H)^2/4\pi\alpha$, one obtains

$$(R - 2x)\, \beta'' - 3\beta' - S\beta = 0 \qquad \ldots(20)$$

Substituting $R - 2x = 2\xi^2$ and $\beta = \nu/\xi$, this reduces to the form

$$\frac{\partial^2 \nu}{\partial \xi^2} - 2S\nu = 0 \qquad \ldots(21)$$

which has the solution

$$\nu = C_1 \cosh \sqrt{2S}\ \xi + C_2 \sinh \sqrt{2S}\ \xi \qquad \ldots(22)$$

or resubstituting

$$\theta = \left(\frac{R - 2x}{2}\right)^{-\frac{1}{2}} \left[C_1 \cos \sqrt{S(2x - R)} + C_2 \sin \sqrt{S(2x - R)}\right] \quad \ldots(22')$$

The first and second boundary conditions (15) give the following Equations (23) and (24); and (22') inserted into the original Equation (14) gives Equation (25). We use the notation $\gamma = \sqrt{-S/4\pi\alpha}$ and keep in mind that $\frac{1}{2}(R - 2x_o) = B_o^2 / 8\pi\alpha$.

$$\frac{B_o \cdot D}{\sqrt{8\pi\alpha}} = C_1 \cos B_o\gamma + C_2 \sin B_o\gamma \quad \ldots(23)$$

$$0 = C_1 \cos (B_o + H)\gamma + C_2 \sin (B_o + H)\gamma \quad \ldots(24)$$

$$0 = C_1 \sin B_o\gamma - C_2 \cos B_o\gamma \quad \ldots(25)$$

These are three equations for the unknowns C_1, C_2 and H. Since we are only interested in H, we write Equation (24) as

$$0 = (\cos H\gamma)(C_1 \cos B_o\gamma + C_2 \sin B_o\gamma) - (\sin H\gamma)(C_1 \sin B_o\gamma - C_2 \cos B_o\gamma) \quad \ldots(24')$$

After substitution of Equation (23) and (25), there remains

$$\frac{B_o \cdot D}{\sqrt{8\pi\alpha}} \cos H\gamma = 0 \quad \ldots(26)$$

and the first solution of (26) gives after replacing $\gamma = \sqrt{-\frac{\partial\alpha}{\partial T} / c4\pi\alpha}$

$$H_{fi} = \frac{\pi}{2} \sqrt{\frac{-4\pi c\alpha}{\frac{\partial\alpha}{\partial T}}} \quad \ldots(27)$$

We may insert the most common temperature dependence of flux pinning

$$F_{P(T)} = F_{P(o)} \left[1 - (T/T_c)^2\right]^2 \qquad \ldots(28)$$

where T_c is the critical temperature. Equation (28) is a fair approximation in many measured cases.[4] It is also plausible if one recalls that pinning is expressed by the local gradient of variations in mean free energy and the pinning sites are locally fixed. Since the difference in Gibbs free energy between normal and superconductive state, being proportional to the square of the critical field, has the temperature dependence of Equation (28) it is likely that the variations also follow this dependence.*

With Equations (28) and (17) one obtains

$$\frac{\partial \alpha}{\partial T} = \alpha(T)\ 4\ T/(T_c^2 - T^2) \qquad \ldots(29)$$

Using (29) in (27) one gets

$$H_{fi} = \frac{\pi}{2} \sqrt{\pi c (T_c^2 - T^2)/T} \qquad \ldots(30)$$

This equation is remarkable as it contains only the specific heat and the critical temperature and neither the pinning strength parameter α nor the rate of change of the external field dH/dt.

Subject to the assumptions of isothermal conditions (dH/dt not too large), semi-infinite half space (good approximation as long as the shielding layer does not reach the center of the specimen), and ordinary field and temperature dependence of flux pinning, the stability limit is expressed by Equation (30).

Formulas similar to (27) and (30) have been presented earlier.[31,32] Without allowing for the influence of η in Equation (3), they were, however, erroneously attributed to H_{fj}.

*This is often not the case if the variations are caused by alloy phases or inclusions which represent superconductors different from the matrix, such as in the Pb-Sn and Pb-Sn-In alloys reported by Livingston.[25]

D. LIMITED INSTABILITY

Once the stability limit as determined by Equation (14) is exceeded then the original equilibrium equation (3) has to be considered in order to study the process initiated by a disturbance. The time derivative of (3) gives an equation of motion for the flux structure

$$\frac{\partial F_L}{\partial t} - \frac{\partial F_P}{\partial t} = \eta \frac{\partial v}{\partial t} + v \frac{\partial \eta}{\partial t} \qquad \ldots(31)$$

This equation has to be valid for all x and t. In addition, the following equation for the conservation of the flux, which enters through the surface, must be fulfilled

$$B \cdot v = \int_{B=0}^{B} \frac{\partial B}{\partial t} \cdot dx \qquad \ldots(32)$$

which gives

$$- \frac{\partial B}{\partial t} = \frac{\partial Bv}{\partial x} = B \frac{\partial v}{\partial x} + v \frac{\partial B}{\partial x} \qquad \ldots(33)$$

in which the sign is negative because $x(B) < x\ (B = 0)$.

Now each of the two terms on the left in (31) have to be worked out.

Making use of (2), (33), one gets

$$\frac{\partial F_L}{\partial t} = \frac{1}{4\pi} \left[B \frac{\partial^2 B}{\partial x \partial t} - v \left(\frac{\partial B}{\partial x} \right)^2 - B \frac{\partial v}{\partial x} \cdot \frac{\partial B}{\partial x} \right] \qquad \ldots(34)$$

This equation can be simplified by making some approximations. As long as $\int v\ (x_o)\ dt \ll x_o$ one can neglect $\partial v/\partial x$ (see Figure 4). The differential quotient in the first term in (34) then becomes

$$\frac{\partial}{\partial t} \left(\frac{\partial B}{\partial x} \right) = -v \frac{\partial^2 B}{\partial x^2}$$

because

$$\frac{\partial B}{\partial x}(x,\ t + \Delta t) = \frac{\partial B}{\partial x}(x - v\Delta t,\ t)$$

with this approximation (34) becomes

$$\frac{\partial F_L}{\partial t} = -\frac{v}{4\pi}\left[\left(\frac{\partial B}{\partial x}\right)^2 + B \cdot \frac{\partial^2 B}{\partial x^2}\right] \qquad \ldots(34')$$

If $\int v dt$ is comparable to x_o, we can make the following approximation (see Figure 16).

1. $\int v\ (x = 0)\ dt = \frac{1}{2} \int v\ (x_o)\ dt$ and therefore $v(x) = \frac{1}{2}\ v\ (x_o)\left[1 + \frac{x}{x_o}\right]$, and $\frac{dv}{dx} = \frac{v(x_o)}{2\ x_o} = \frac{v}{x_o + x}$

and

2. $\frac{\partial B}{\partial x} = P(x)\ \frac{H}{x_o}$ where P is a proportionality constant. Then

$$\frac{\partial}{\partial t}\left(\frac{\partial B}{\partial x}\right) = \frac{\partial}{\partial t}\left(P\ \frac{H}{x_o}\right) = -\frac{PH}{x_o^2} \cdot \frac{\partial x_o}{\partial t} = -\frac{\partial B}{\partial x} \cdot \frac{v(x_o)}{x_o} = -\frac{\partial B}{\partial x}\ \frac{2v}{(x_o + x)}$$

Now (34) becomes

$$\frac{\partial F_L}{\partial t} = -\frac{v}{4\pi}\left[\left(\frac{\partial B}{\partial x}\right)^2 + B\ \frac{\partial B}{\partial x}\ \frac{3}{x_o + x}\right] \qquad \ldots(34'')$$

The difference between (34), (34'), and (34'') is usually insignificant because $(\partial B/\partial x)^2$ is very large.

For the pinning force term in (31) one gets

$$\frac{\partial F_P}{\partial t} = \frac{\partial F_P}{\partial T} \cdot \frac{\partial T}{\partial t} + \frac{\partial F_P}{\partial B} \cdot \frac{\partial B}{\partial t} \qquad \ldots(35)$$

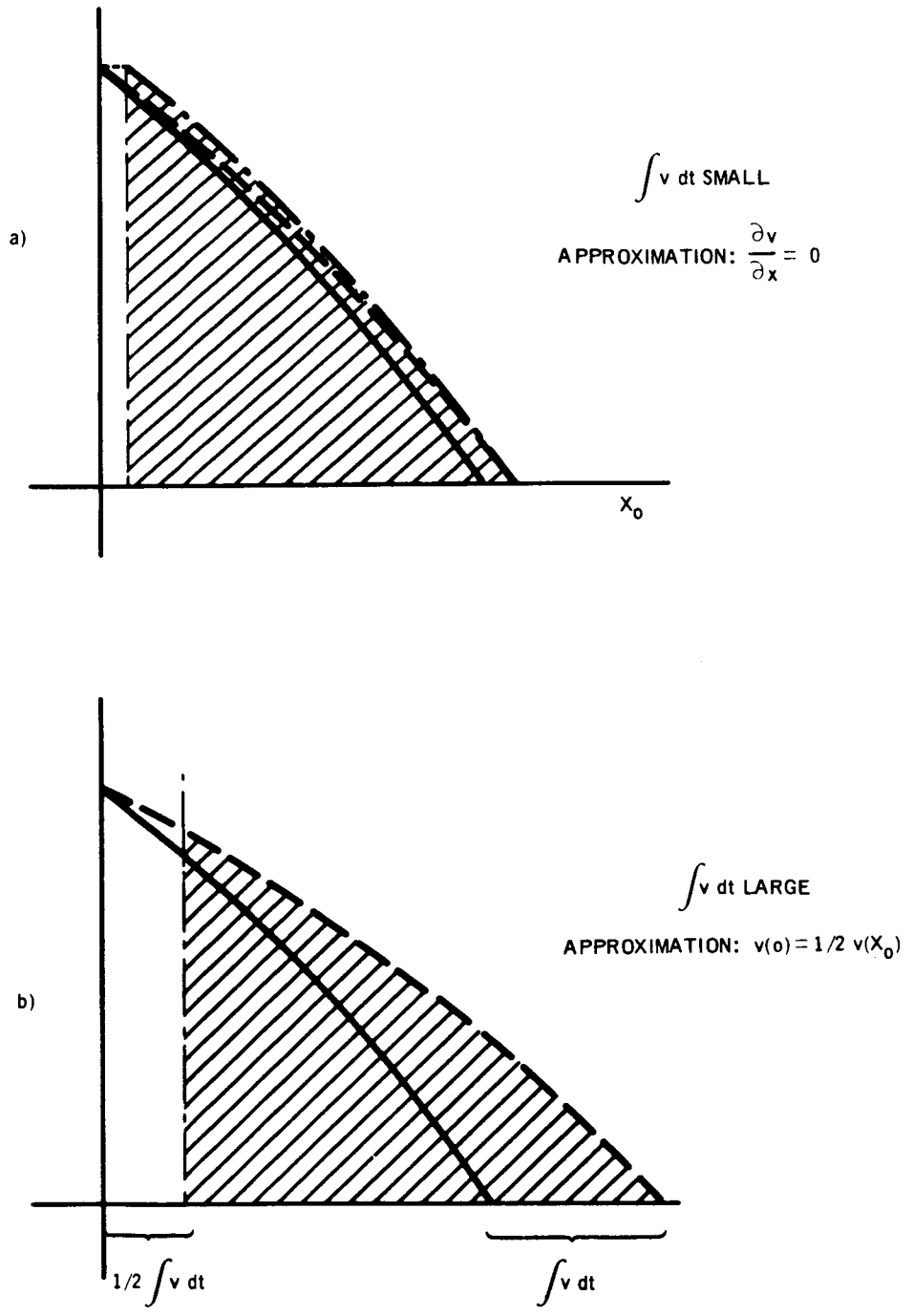

Figure 16. Approximations Concerning the Speed of the Flux Structure. The shaded area indicates where the flux of the original penetration layer is found after the disturbance. The triangle with $\int$ vdt as a base is equal in area to the rectangle with $\frac{1}{2} \int$vdt as a base.

The temperature is again given by a solution of the heat equation (12). Instead of (11), we write

$$\int \frac{\partial T}{\partial t}\, dt = f\, \frac{1}{c} \cdot \int \frac{\partial q}{\partial t}\, dt \qquad \ldots(36)$$

Where $f = f(x,t,dq/dt)$ is a parameter measuring the steadiness of the temperature distribution according to Equation (12) [f (adiabatic) = 1, f (steady state) = 0]. See also Figure 17.

If we neglect the change in shielding current, we get [cf. Equation (10)]

$$\frac{\partial q}{\partial t} = j \cdot \frac{\partial \Phi}{\partial t} = j\, v\, B = \frac{1}{4\pi}\, v\, B \cdot \frac{\partial B}{\partial x} \qquad \ldots(37)$$

with the use of (33), (35) then becomes

$$\frac{\partial F_P}{\partial t} = - \frac{\partial F_P}{\partial T} \left[\alpha_{th} \frac{\partial^2 T}{\partial x^2} + \frac{j}{c}\, v\, B \right] + \frac{\partial F_P}{\partial B} \left(B \frac{\partial v}{\partial x} + v \frac{\partial B}{\partial x} \right) \qquad \ldots(38)$$

If we make use of the notation (36)

$$\frac{\partial F_P}{\partial t} = - \frac{\partial F_P}{\partial t} \cdot f \frac{j}{c}\, v\, B + \frac{\partial F_P}{\partial B} \left(B \frac{\partial v}{\partial x} + v \frac{\partial B}{\partial x} \right) \qquad \ldots(38')$$

We can now write the original equation (31), replacing η with $c_\eta B$, as follows, for small v

$$- \frac{v}{4\pi} \left[\left(\frac{\partial B}{\partial x} \right)^2 + B \frac{\partial^2 B}{\partial x^2} \right] + \frac{\partial F_P}{\partial T} \frac{f}{4\pi C} \frac{\partial B}{\partial x} vB + \frac{\partial F_P}{\partial B}\, v \cdot \frac{\partial B}{\partial x} = c_\eta \left(B \frac{\partial v}{\partial t} - v^2 \frac{\partial B}{\partial x} \right) \qquad \ldots(39)$$

Which has the form

$$\frac{\partial v}{\partial t} = a_i\, v + b_i\, v^2 \qquad \ldots(40)$$

where

$$a_1 = \frac{1}{B\, c_\eta}\left[\frac{\partial F_P}{\partial B} \cdot \frac{\partial B}{\partial x} - \frac{B}{4\pi}\frac{\partial^2 B}{\partial x^2} - \frac{1}{4\pi}\left(\frac{\partial B}{\partial x}\right)^2 - \frac{f}{c} \cdot F_P \cdot \frac{\partial F_P}{\partial T}\right] \qquad \ldots(41)$$

and

$$b_1 = \frac{1}{B} \cdot \frac{\partial B}{\partial x} \cdot$$

For larger v, Equation (40) must be written, replacing a_1 and b_1 with

$$a_2 = \frac{1}{B\, c_\eta}\left[\frac{\partial F_P}{\partial B}\left(\frac{B}{x + x_o} + \frac{\partial B}{\partial x}\right) - \frac{B}{4\pi}\frac{\partial B}{\partial x}\frac{3}{x + x_o} - \frac{1}{4\pi}\left(\frac{\partial B}{\partial x}\right)^2 - \frac{f}{c} \cdot F_P \cdot \frac{\partial F_P}{\partial T}\right]$$

$$\ldots(41')$$

$$b_2 = \frac{1}{B} \cdot \frac{\partial B}{\partial x} + \frac{1}{x + x_o}$$

Equation (40) is solved by

$$v = -\frac{a_i}{b_i}\left[C\, e^{-a_i t} + 1\right]^{-1} \qquad \ldots(42)$$

Where C is given by the initial speed v_o

$$C + 1 = -\frac{a_i}{b_i\, v_o} \qquad \ldots(43)$$

C being a large number, the addition of 1 can usually be neglected. For small t (42) can therefore be written

$$v = v_o\, e^{a_1 t} \qquad \ldots(44)$$

(44) applies as long as $\int v\,dt \ll x_o$, i.e., in almost the whole limited instability range.

Note that for $v_o = 0$, the solution of (40) is $v \equiv 0$ as is seen in (44). This is expected since $v_o = 0$ implies no disturbance and the system was originally in equilibrium.

It is further seen from Equation (44) that v decreases for $a_1 < 0$ and $v = v_o$ = constant for $a_1 = 0$, i.e., a disturbance will stop by itself and the equilibrium is stable, $a_1 = 0$ giving the limit of stability. Indeed Equation (14) which was given as the stability limit in the previous section will give the same result if the time derivative is formed, using the simplifications introduced after Equation (34) and keeping in mind that $\partial\beta/\partial t = \partial B/\partial t$ and $f = 1$.

It has been mentioned above that a limited instability is characterized by a period of acceleration, followed by deceleration. The time interval following a disturbance in which the maximum speed is reached may be called t_m. By comparison with Equation (40), v is a maximum when

$$a_i (t_m) = - b_i v \qquad \ldots(45)$$

If a_i and b_i were constant, this, according to (42), has only a solution for $t_m \to \infty$, thus the maximum speed would become

$$v (t = \infty) = - \frac{a_i}{b_i} \qquad \ldots(46)$$

However, a_i is a function of x and also of f which is itself dependent on x and t.

An exact treatment would require that Equation (31) be solved simultaneously for all x and t, inserting the heat equation correctly. This would lead to a differential equation for the shape of the disturbance similar to (14), only more complicated. The solution would give the true v (x,t) describing the complete process of a limited instability. Needless to say, this would be an enormously difficult task, quite outside the scope of the present study and, in the absence of precise experimental data, unwarranted.

Instead, having already, by assuming dv/dx = o, ignored the dependence of v on x, we shall continue with the adoption of a great simplification concerning

the heat equation. The results of the subsequent discussions and calculations will therefore be more of a qualitative nature. However, the recipes for estimating the maximum speed during a limited instability and the field at the beginning of runaway instabilities should amply justify the procedure.

After this short apology, we can now show generally, by considering f, that the quantity a_i, starts decreasing after a very short time, passes through zero (shortly after t_m) and becomes negative. The connection between f and a_i is seen from Equations (41) and (41') which, however, are correct only for very short times or f = 1. At the beginning, f is unity in the whole shielding layer except at the boundary where f is kept close to zero by the cooling of the liquid helium through the surface and by radiation into the bulk at x_o. With increasing time, f will decrease gradually throughout the layer because of heat conduction to the boundaries. Figure 17 gives an illustration of f for the case of dq/dt = constant and $t > o$, $o < x < x_o$, with the reduced time variable $t\alpha_{th}/d^2$ as a parameter, where α_{th} is the thermal diffusivity and d ($= x_o$), the thickness of the layer. In this figure, only the values at the center have been calculated, assuming that both surfaces of the plane slab are kept at zero temperature. The remainder has been filled in by approximating, for small time values, by the unsteady state solution and, for large t, by the steady state solution of the heat equation. The left hand boundary is assumed to stay at zero temperature and at the right-hand boundary there is radiation into the same medium at zero temperature. This would make f infinite at the boundary itself, which is the reason for leaving the vicinity of x_o blank.

We learn from Figure 17 that for $t\alpha_{th}/d^2 < 0.02$ the assumption f = 1 is a fair approximation and that for longer times f reduces rapidly.

If one can neglect the change in x_o during the whole limited instability process [see Equation (34')], one writes t_m from Equation (45) as

$$t_m = \frac{x_o^2}{\alpha_{th}} \cdot g_1 \qquad \ldots(47)$$

Seeing that f is small at the surface and near x_o and without knowing the exact shape of the disturbance, we can say that the change in the shielding

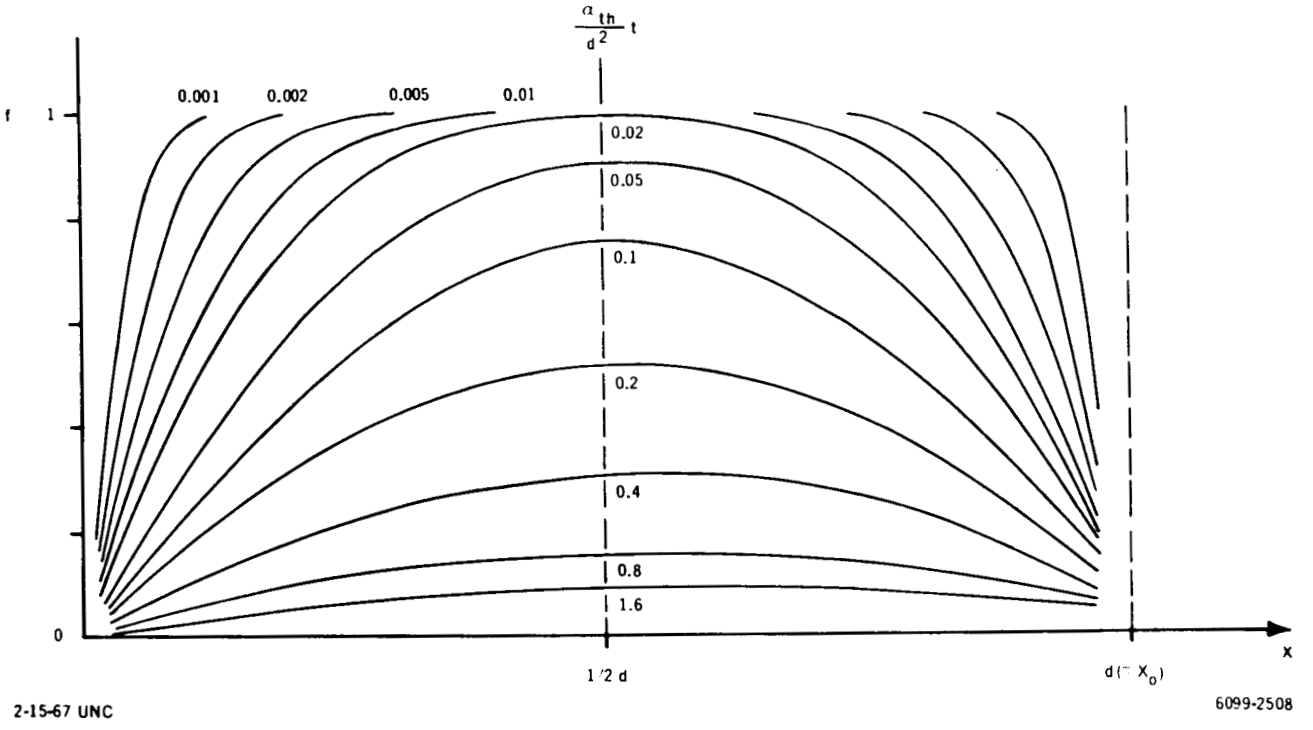

Figure 17. Temperature Distribution Function f vs x in the Penetration Layer, for Increasing Time Parameters $\theta = \alpha_{th}\, t/d^2$. $f = \Delta T\, c/_o\int^t dq/dt\, dt$, where $\Delta T = T - T_{surface}$. Formulae for ΔT are found in Reference 33. In the present case f for x = d/2 and dq/dt = constant, has been computed as $f = 1/m \sum_{i=o}^{m} S(\theta \cdot [1 - i/m])$, m being a large number. The function $S(\theta)$ is tabulated in Reference 34.

layer, i.e., the change in B and dB/dx is largest near the center. One might also say that the acceleration force is largest at the center and is spread out over the whole of the layer because of the elastic rigidity of the flux structure. Considering all this, one may make a plausible choice of $g_1 = 0.015$, which is the value for which f at the center starts to diminish. With this, Equation (44) can be written

$$v_{max} = \frac{H}{4\pi F_p(H)} \cdot \frac{dH}{dt} \exp\left(0.015\, a_i\, x_o^2/\alpha_{th}\right) \qquad ...(48)$$

In this formula, v_o has been replaced by v_{dr} from Equation (4) using Equations (2) and (6).

E. RUNAWAY INSTABILITY OR FLUX JUMP

We have seen that, once the stability limit is exceeded, a disturbance will cause the flux lines to be accelerated by the Lorentz forces because of the weakening of the flux pinning. The velocity, starting from the drift velocity, will eventually reach a maximum value. In the case of a limited instability, this value is comparatively low, allowing a thermal recovery of the bulk of the shielding layer via heat conduction. Thus, the pinning forces recuperate and a deceleration of the flux structure sets in which stops the instability again. Thermal recovery starts when the time parameter $\alpha_{th}\, t/d^2$ reaches a certain critical value, which from a study of Figure 17 we have guessed to be 0.015.

The situation may change when the thickness, d, of the shielding layer

$$d = x_o + \int v dt \qquad ...(49)$$

increases noticeably during the acceleration period. Should d grow faster than $\sqrt{t}$, we obtain a case where the thermal time parameter decreases with increasing time, t. This means that the heat conduction is too slow and the process becomes, or remains, adiabatic; i.e., the thermal function f = 1 [see Equation (36) and Figure 17].

In this kind of process, the acceleration continues until a final runaway speed is reached. Naturally in due course the movement terminates owing to the boundaries of the superconductor.

This process is a flux jump and it occurs when the following criterion holds

$$\alpha_{th}\, t/d^2 \leq g_2 \qquad \ldots(50)$$

In other words: the condition for the development of a runaway instability is that the thermal time parameter, which is zero to begin with, will not exceed a certain critical value, g_2, because of the expansion of the thickness of the shielding layer.

In order to make a quantitative estimate, we shall adopt the same recipe as in the previous section. We assume that Figure 17 is a reasonable approximation for the function f, although as d is not constant the agreement would be expected to be somewhat poorer. This would again give a choice of $g_2 = 0.015$.

We arrive at the threshold value for a runaway instability by putting this critical value into Equation (50) and assuming the equality sign. Since $f = 1$ is again valid, we can use Equations (40)-(44) in determining v which gives the value for d according to Equation (49).

We still have to decide what limits the integral in Equation (49) should take. The obvious choice of taking v_{dr} as the initial speed is not good if we realize that Figure 17 is only right for constant dq/dt which in this case means constant v. Instead of being constant, v changes by several orders of magnitude before the integral becomes comparable to x_o. Therefore, the insertion of the initial speed v_{max} from Equation (48) is suggested. Thus the thermal time parameter is counted from the moment when the heat production has reached this almost constant, higher level of the limited instability.

On the basis of these considerations, the formal result is reached as follows. Taking v from the expression (42), the constant C assumes the value

$$C = -\left(\frac{a_i}{b_i\, v_{max}} + 1\right) \qquad \ldots(51)$$

where v_{max} is given in (48). With

$$\int_0^t v\,dt = -\frac{a_i}{b_i}\,t - \frac{1}{b_i}\log\left(1 + C\,e^{-a_i t}\right) \qquad \ldots(52)$$

The criterion Equation (50) becomes

$$x_o\,t^{-\frac{1}{2}} - \frac{a_i}{b_i}\,t^{\frac{1}{2}} - \frac{t^{-\frac{1}{2}}}{b_i}\log\left(\frac{1 + C\,e^{-a_i t}}{1 + C}\right) = \sqrt{\frac{\alpha_{th}}{0.015}} \qquad \ldots(53)$$

The condition that the left-hand side shall be a minimum will determine the unknowns t and C. The constant C contains the value H_{fj}, the threshold field for runaway instability.

In a practical evaluation, one may get the left-hand side of (53) vs. time directly from Equation (40) by means of an analog computer.

F. CONCLUSION

In order to appreciate the applicability of the formulas presented in the previous chapters, it is of importance to state once more clearly the assumptions made and discuss the effect of deviations from them. In subsequent sections, the influence of the main variables, such as dH/dt, α_{th}, F_P and $\partial F_P/\partial T$, will be outlined and finally, a comparison in a general way with experimental findings should be of interest.

Magnetic instabilities can only occur when a superconductor is not in thermodynamic equilibrium, i.e., irreversible. Terms like "perfect" or "ideal" allude to a high degree of reversibility;[35] an "ideal" superconductor cannot sustain any macroscopic magnetic gradients in the mixed state.[36-38] The maximum of the deviation from equilibrium which an imperfect superconductor is capable of can be characterized by a "critical state." This, for the purpose of the present investigation, is sufficiently described by a bulk critical current density J_c which is normally a function of the local induction B and temperature T. In general, and recently the subject of various studies,[39] there is also a surface critical current density J_{cs} - in addition to the equilibrium surface current responsible for the ideal diamagnetic properties of the superconductor, and unlike this one it can have positive or negative sign. Maxwell's equations

allow an alternative description of the critical state in terms of a magnetic gradient $\partial B/\partial x = 4\pi J_c$ and of a step at the surface $\Delta H_s = 4\pi J_{cs}$. A third equivalent description uses pinning forces which are connected to the previous two views by being the reaction to the Lorentz force, $F_P = J_c \times B$; in this more microscopic picture the surface current takes the role of a surface barrier.[40]

While in many magnetically unstable superconductors these surface currents are not negligible, (ΔH_s is of the order of 100 gauss in NbZr and NbTi[41]), their influence on the instability problem is small if the surface is well cooled as in our conditions. Naturally the boundary field which the bulk flux structure sees should be taken as $H - \Delta H_s$ rather than the external field H alone. Since instabilities related to the surface represent sudden changes of ΔH_s, they become a source of disturbances similar in effect to an unsteady dH/dt.

We have assumed isothermal conditions; this is largely a mathematical convenience. The same physical ideas apply when dH/dt is too large for the isothermal approximation, but simplifications like Equations (4) and (16) are no longer allowed and the calculation may become prohibitively complicated. For large values of dH/dt one approaches fully adiabatic conditions. Then a very simple criterion will establish an upper limit for the flux jumping field,[42] however, the presently outlined mechanism may, and usually does, still cause instabilities at a slightly lower field.

An important simplification justified by the isothermal assumption is the heat equation (12). In this form it is only valid when the thermal diffusivity is a constant. In reality $\alpha_{th} = K/c$ is a function of T because both c and K vary differently with temperature. The correct heat equation

$$c \frac{\partial T}{\partial t} = \nabla(K \nabla T) \qquad \ldots(54)$$

becomes

$$\frac{3}{2} \epsilon \frac{\partial(T^4)}{\partial t} = \zeta \nabla^2 (T^3) \qquad \ldots(55)$$

if $c = \epsilon T^3$ and $K = \zeta T^2$ which are fairly close to the actual functions in the superconductor.

In adopting Equation (11), we have also assumed that the magnetic diffusivity is larger than the thermal diffusivity. In reality the magnetic disturbance, β in Equation (10), is itself the result of a diffusion process and should likewise be the solution of an equation

$$\frac{\partial \beta}{\partial t} = \alpha_{el.mag.} \beta'' \qquad \ldots(56)$$

This is important because $\alpha_{el.mag.}$ is proportional[28] to dH/dt; consequently, for small dH/dt, the disturbance propagates itself so slowly that Equation (11) is never valid, the heat being conducted away as it is produced. Equation (56) was used to determine the stability limit in dependence of dH/dt by means of an analog computer, but the results depend on the type of magnetic disturbance being used as a boundary condition and, moreover, $\alpha_{el.mag.}$ far from being a constant, renders Equation (56) a very poor approximation for similar reasons as given above in discussing the heat equation.

In the present treatment dH/dt enters through v_{dr} of Equation (4) into Equation (48) to influence the limited instability and H_{fj}; because of (10) the stability limit is independent of dH/dt, thus for very small dH/dt the results are questionable.

In connection with the drift velocity, it should be pointed out that for very slow movements v_{dr} represents an average speed which may be composed of short quick movements of individual vortices while the others are stationary. Spacing of pinning sites may be of the order of 10^{-5} cm which is the same as the spacing of fluxoids at B = 2000 G. With the idea of spatially discreet pinning centers and the elasticity of the flux structure[43] (Maxwell tensor), one might assume that a small section of a flux line having cleared a pinning site moves a fraction of this distance, say 10^{-6} cm. If $v_{dr} < 10^{-6}$ cm/sec (for $j = 10^6$ A/cm^2, dH/dt < 10 Oe/sec) then this process occurs only once every second. This is also a reason why for very low v_{dr} the present treatment is poor and why Equation (56) is no big improvement.

This, lastly, raises the question of the validity of a constant viscosity η in Equation (3). The nonlinearity of Equation (3) has been experimentally investigated[44] and it was found that for $F_L < F_P$ the drift velocity reaches

finite values. In the light of the above model and in order to keep the formalism of Equation (3) intact one would have to add to the Lorentz force a force, F_{def}, which is due to the deformation of the flux structure. F_{def} expresses the excess of the steepest local gradient over the average gradient dB/dx connected [Equation (2)] with F_L. Equation (3) then becomes

$$F_L = F_P - F_{def} + \eta v \qquad \ldots(57)$$

F_{def}, according to the results of Reference 44, can be expressed as a function of F_L/F_P and would take values as illustrated in Figure 18. v (which can only be positive) is different from zero when

$$\frac{F_{def}}{F_P} \geq 1 - \frac{F_L}{F_P} \qquad \ldots(58)$$

Our criterion of instability as given in (7) or (31) can also be written as

$$\frac{\partial}{\partial t}\left(\frac{F_L}{F_P}\right) > 0 \qquad \ldots(59)$$

but with (59) we have because of (58) also

$$\frac{\partial}{\partial t}\left(\frac{F_L}{F_P - F_{def}}\right) > 0 \qquad \ldots(60)$$

Consequently, the criterion for stability is unaffected by this more refined description. Once the stability limit is exceeded one has to expect a lower v_{max} speed during a limited instability. This in turn leads to a higher runaway field H_{fj}. At present not enough is known about F_{def} and since its relative size ($\sim$ 20%) compares with the scattering of experimental flux jumping data, the mathematical complications are a strong bias against its inclusion.

The geometric assumption of a semi infinite plane superconductor is not very restrictive because in most cases the shielding layer thickness d is small compared to the dimensions of the superconductor. Conversion of the calculation into cylindrical coordinates shows that for d < 80% of radius r of a solid

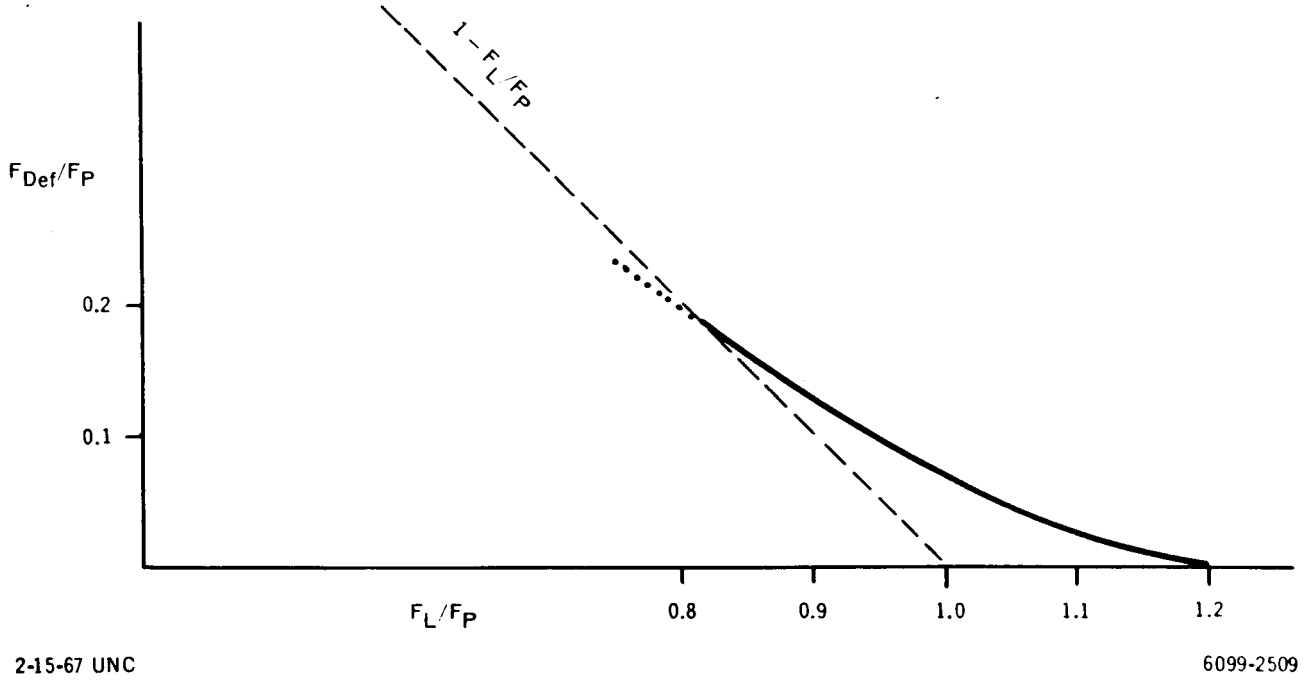

Figure 18. Qualitative Illustration of F_{def}/F_P vs F_L/F_P on the Basis of Reference 44

cylinder, the change is very small. If the shielding layer grows further towards the center then the danger for instabilities subsides as outlined in the second chapter, Figure 14c.

Cooling in zero field has been taken as an initial condition with regard to the magnetic history of a specimen. Normally after a flux jump, B inside is uniform and equal to H ($= H_{fj}$) outside,[15] in which case subsequent instabilities can be worked out by applying the same formalism unchanged except for the initial field H which becomes H_{fj} instead of zero. Neither does it matter whether, after a flux jump, the field is raised or lowered; if B = 0 is crossed, some small complications, mentioned in detail later, may arise. In general and for more complicated magnetic histories, it is sufficient to know the (macroscopic) distribution of B throughout the shielding layer in order to easily adapt the given formulas.

In this context the case of the external field being not parallel to the surface should be mentioned. Again if the internal distribution of B is known the present treatment should, in principle, be adaptable. The difficulty in predicting B in such cases seems at present at least as big an obstacle as the anticipated mathematical complexity. This has been discovered recently for the simple geometry of a long cylinder in a perpendicular field.[45,46]

For the brief discussion of the influence of variables on the results, we shall stay within the assumptions originally adopted and we include external variables such as H, dH/dt and T as well as material constants such as F_p, $\partial F_p/\partial T$, α_{th}, c.

It may be repeated here that in regions (with regard to T and H) where $\partial F_p/\partial T > 0$ the stability limit (7) or (58) is never reached and the superconductor is inherently stable. A small argument has been presented which makes plausible why many defects have a pinning strength which decreases with increasing temperature like $(1 - [T/T_c]^2)^2$ but there are many pinning mechanisms possible and there have been reports of $\partial F_p/\partial T > 0$.[6,30,47]

The variation of the stability limit as $c^{\frac{1}{2}}$ is seen directly from (27) and (30). Many studies[14,48,49] have suggested, at least qualitatively, similar formulas containing the $c^{\frac{1}{2}}$ dependence. Since H_{fj} is more or less proportional to H_{fi} the influence of c is reflected in the flux jumping field. Experiments

with porous Nb_3Sn give a good illustration.[49-51] If the pores are filled with liquid helium, c being the specific heat per unit volume will have a contribution from the heat of vaporization of the liquid, which for completely isothermal conditions can increase c by a factor of 100, increasing H_{fj} tenfold.

The effect of the actual size of F_p is weak, having no influence on the stability limit [Equation (30)]. Weak pinners, however, often do not fulfill the geometric assumption of infinite thickness and appear therefore more stable. F_p enters Equation (48) and thus influences H_{fj} in Equations (51)-(53). H_{fj} changes in the same sense as F_p. (See specimen 4 in Reference 42.) The influence of dH/dt is very similar but inverse to that of F_p, as seen in (48). For large dH/dt, H_{fj} will reach a constant value considerably above H_{fi}, for small dH/dt, H_{fj} increases logarithmically.[52]

The thermal diffusivity has also a comparatively weak influence, changing H_{fj} in the same sense. The temperature dependence of α_{th} being close to T^{-1} tends to counteract the $(1 - [T/T_c]^2)^2$ dependence of F_p, resulting in a weak temperature dependence of H_{fj} in spite of the variation of H_{fi}.[53]

Finally, we try to find experimental illustration and confirmation of the presented arguments and calculations. Although magnetic instabilities have frequently been observed, they are usually not in the focal point of an investigation and therefore only incidentally reported. Often the geometries are remote from the plane slab, or the material of an inhomogeneous nature, the results therefore only qualitatively comparable.

The present study has partly been stimulated by an experimental investigation of flux jumping in solid NbZr cylinders. Some of the results have been reported[42] and a more detailed description including measurements of α_{th}, $\partial F_p/\partial T$, and incorporating calculations as outlined here will be published elsewhere. The agreement of these results with the present theory is reasonable; naturally, the choice of the critical constants g_1 and g_2 has been influenced by these experimental results.

Perhaps insufficiently recognized so far is the fact that runaway instabilities are preceded by limited instabilities. The latter often go unnoticed in experiments which measure flux jumping activities because the effect in terms of change in magnetization or amount of flux involved is very much smaller.

However, experiments by Wischmeyer[54] clearly show small rushes of flux, of 100 flux quanta or more, which increase with dH/dt and are observed under conditions which immediately precede the occurrence of flux jumps and above the stability limit. Another interesting observation is that these limited instabilities are, as expected, also localized with regard to the specimen surface.[55]

Further observations of limited instability have been reported as "flux jumps" of between 5×10^4 and 2×10^7 quanta each where a total flux jump would require at least 10^8 quanta.[56] The magnetocaloric effect reported by Zebouni, et al.,[57] can almost certainly be attributed to limited flux jumping.

It must be pointed out here that a series of limited instabilities can lead to a sufficient relaxation of the Lorentz force, so that real runaway instabilities never occur.

Since the solution of Equation (40) gives a final velocity v_∞ [see Equation (46)] and since there are various measurements of such velocities,[45,58,59] we ought to focus our attention quickly on this point. If during a flux instability a final velocity is reached, it will be given by an integral of Equation (31), similar to Equation (46). Of course, neither a_i nor b_i is constant. Such a solution would be expected to give smaller speeds than a solution of the diffusion equation

$$\frac{\partial^2 H}{\partial x^2} = 4\pi\sigma \frac{\partial H}{\partial t} \qquad \ldots(61)$$

with σ being the normal electrical conductivity. However, in the adiabatic flux jumping limit equation (61) could apply. We can therefore say that for flux jumps occurring below H_A of Reference 42 the final speed will be lower than a solution of (61) and depend on H_{fj}. If $H_{fj} \geq H_A$ (for small dH/dt, higher temperatures, etc.) then Equation (61) will apply.

The question of what happens after the runaway speed has been reached has not been treated here. We mentioned earlier that most observed flux jumps end when flux has reached the center of the specimen; but even in the semi infinite slab the movement will come to a rest since the runaway speed is not infinite and thermal recovery does take place behind the moving flux front. Thus the

recovering flux pinning will interrupt the supply of flux. An excellent experimental study by Wertheimer and Gilchrist[60] shows this in the case of very short cylinders.

It has been noticed in certain experiments that, immediately after a flux jump, no or very little flux is admitted. This indicates the influence of the surface critical current and is especially noticeable when ΔH_s is comparable to $dB/dx \cdot r$, which is normally the case for low κ material like Nb[61] or for weak pinners like Pb-Bi alloys. In this context another influence has recently come to notice; it was reported[62] that what must be surface originating instabilities occur under otherwise equal stability conditions only when flux is leaving the sample but not when entering. In this particular case the entropy of the flux lines,[63] needed to create the fluxoids when entering the sample and set free when fluxoids leave, will create a change of the surface temperature of $\sim 1 \times 10^{-3}$ °K.* This temperature change being negative when fluxoids enter the specimen stabilizes ΔH_s, being positive when fluxoids leave, it adds to the Joule heating, thus increasing the instability conditions.

It has been suggested that the annihilation of flux lines in the region where $B = 0$ is a crucial influence in causing flux jumps.[12,63,64] But in many cases such an influence can hardly be noticed.[51,53] The annihilation of flux lines which will release additional energy will doubtlessly complicate the picture in the region $B = 0$ along with the possibility of a Meissner state (for $B < H_{c1}$) and consequently an intermediate state between the regions of opposing flux; but fortunately in most cases the influence is negligible.

*Note that in Reference 62 there is an error concerning the diameter of the specimen which should be 34 mil (= 0.86 mm) and not 34 mm as printed (private communication by J. Silcox). To arrive at the surface temperature change, we used heat transfer values extrapolated from Reference 22.

ACKNOWLEDGMENTS

The author thanks A. G. Presson for solving some computer problems and M. S. Lubell, H. T. Coffey, H. J. Fink, and T. G. Berlincourt for helpful discussions.

REFERENCES

1. M. Hansen, E. L. Kamen, H. D. Kessler, and D. J. McPherson, Trans. AIME, 191, 881 (1951).

2. J. O. Stiegler, J. T. Houston, and M. L. Picklesimer, J. Nuc. Mat., 11, 32 (1964).

3. H. G. Van Bueren, "Imperfections in Crystals," North-Holland Pub. Co., Amsterdam (1961), p. 280.

4. S. L. Wipf, paper presented at the Conference on Type II Superconductors, Cleveland (1964); Westinghouse Scientific Paper 64-1JO-280-P1.

5. T. G. Berlincourt and R. R. Hake, Phys. Rev., 131, 140 (1963).

6. J. Sutton and C. Baker, Phys. Letters, 21, 601 (1966).

7. Y. B. Kim, C. F. Hempstead, and A. R. Strnad, Phys. Rev. 129, 528 (1963).

8. P. S. Swartz and C. H. Rosner, J. Appl. Phys. 33, 2292 (1962).

9. A. F. Hildebrandt, D. D. Elleman, F. C. Whitmore, and R. Simpkins, J. Appl. Phys. 33, 2375 (1962).

10. M. S. Lubell, B. S. Chandrasekhar, and G. T. Mallick, Appl. Phys. Letters 3, 79 (1963).

    H. Riemersma, J. K. Hulm, and B. S. Chandrasekhar, Adv. Cryog. Eng. 9, 329 (1964).

11. C. J. Gorter, Physica, 31, 407 (1965).

12. J. E. Evetts, A. M. Campbell, and D. Dew-Hughes, Phil. Mag. 10, 339 (1964).

13. B. B. Goodman, Rev. Mod. Phys. 36, 12 (1964).

14. P. O. Carden, Aust. J. Phys. 18, 257 (1965).

15. H. T. Coffey, Bull. Am. Phys. Soc. 10, 60 (1965). For more details, see Westinghouse Memo 65-190-CRYOA-M1.

16. K. G. Petzinger and J. J. Hanak, RCA Rev. 25, 542 (1964).

17. C. P. Bean, Rev. Mod. Phys. 36, 31 (1964).

18. W. A. Fietz, M. R. Beasley, J. Silcox, and W. W. Webb, Phys. Rev. 136, A335 (1964).

19. C. J. Gorter, Phys. Letters 2, 26 (1962).

20. W. W. Webb, Phys. Rev. Letters 11, 191 (1963).

G. J. van Gurp and D. J. van Ooijen, paper presented at the Colloque sur la Physique des Dislocations, Toulouse, March 1966. To be published in Journal de Physique.

21. J. Friedel, P. G. de Gennes, and J. Matricon, Appl. Phys. Letters 2, 119 (1963).

22. Y. B. Kim, C. F. Hempstead, and A. R. Strnad, Phys. Rev. 139, A1163 (1965).

23. J. Volger, F. A. Staas, and A. G. Van Vijfeijken, Phys. Letters 9, 303 (1964).

24. J. Bardeen, Phys. Rev. Letters 13, 747 (1964).

25. M. Tinkham, Phys. Rev. Letters 13, 804 (1964).

26. M. J. Stephen and J. Bardeen, Phys. Rev. Letters 14, 112 (1965).

27. A. P. Dorey, Cryogenics, 5, 146 (1965).
A. Karagounis, Bull. Int. Inst. Refrig. Annex 2, 195 (1956).

28. M. S. Lubell and S. L. Wipf, J. Appl. Phys. 37, 1012 (1966).

29. Y. B. Kim, C. F. Hempstead, and A. R. Strnad, Phys. Rev. Letters 9, 306 (1962).

30. J. D. Livingston, Appl. Phys. Letters 8, 319 (1966).

31. S. L. Wipf and M. S. Lubell, Bull. Am. Phys. Soc. 10, 60 (1965). (See also footnote in Reference 42)

32. P. S. Swartz and C. P. Bean, Bull. Am. Phys. Soc. 10, 359 (1965).

33. H. S. Carslaw and J. C. Jaeger, "Conduction of Heat in Solids" (Oxford University Press, Oxford, 1947), Chap. III § 44.

34. L. R. Ingersoll, O. J. Zobel, and A. C. Ingersoll, "Heat Conduction" (University of Wisconsin Press, Madison, 1954), p. 299 ff.

35. The GLAG theory is based on thermodynamic equilibrium. See:

A. A. Abrikosov, Zh. Eksperim. i Teor. Fiz. 32, 1442 (1957) [Translation: J. Phys. Chem. Solids 2, 199 (1957)]

36. C. J. Gorter, Z. Angew. Phys. 14, 722 (1962).

37. W. Klose, Phys. Letters 8, 12 (1964).

38. J. W. Heaton and A. C. Rose-Innes, Appl. Phys. Letters 2, 196 (1963), and Cryogenics 4, 85 (1964).

39. A. A. Abrikosov, Zh. Eksperim. i Teor. Fiz. 47, 720 (1964). [Translation: Soviet Phys., JETP 20, 480 (1965)]

H. J. Fink and L. J. Barnes, Phys. Rev. Letters 15, 792 (1965).

J. G. Park, Phys. Rev. Letters 15, 352 (1965).

40. C. P. Bean and J. D. Livingston, Phys. Rev. Letters 12, 14 (1965).

41. H. A. Ullmaier and W. F. Gauster, J. Appl. Phys. 37, 4519 (1966).

42. S. L. Wipf and M. S. Lubell, Phys. Letters 16, 103 (1965).

43. P. G. de Gennes and J. Matricon, Rev. Mod. Phys. 36, 45 (1964).

44. D. E. Farrell, I. Dinewitz, and B. S. Chandrasekhar, Phys. Rev. Letters 16, 91 (1966).

45. M. S. Walker and J. K. Hulm, Appl. Phys. Letters 7, 114 (1965).

46. Y. Iwasa and J. E. C. Williams, Appl. Phys. Letters 9, 391 (1966).

47. R. R. Hake, T. G. Berlincourt, and D. H. Leslie, Bull. Am. Phys. Soc. 7, 474 (1962).

48. F. Lange, Cryogenics 6, 176 (1966).

49. R. Hancox, Phys. Letters 16, 208 (1965); Appl. Phys. Letters 7, 138 (1965).

50. J. M. Corsan, G. W. Coles, and H. J. Goldsmid, Brit. J. Appl. Phys. 15, 1383 (1964).

51. P. F. Smith, A. H. Spurway, and J. D. Lewin, Brit. J. Appl. Phys. 16, 947 (1965).

52. J. M. Corsan, Phys. Letters 12, 85 (1964).

53. J. H. P. Watson, J. Appl. Phys. 37, 516 (1966).

54. C. R. Wischmeyer and Y. B. Kim, Bull. Am. Phys. Soc. 9, 439 (1964). See also Figure 9 in: Y. B. Kim, Physics Today, September 1964, p. 21-30.

55. C. R. Wischmeyer, Phys. Letters 19, 543 (1965).

56. E. S. Borovik, N. Ya. Fogel' and Yu. A. Litvinenko, Zh. Eksperim. i Teor. Fiz. 49, 438 (1965). [Translation: Soviet Phys., JETP 22, 307 (1966)]

57. N. H. Zebouni, A. Venkataram, G. N. Rao, C. G. Grenier, and J. M. Reynolds, Phys. Rev. Letters 13, 606 (1964).

58. R. B. Flippen, Phys. Letters 17, 193 (1965).

59. B. B. Goodmann and M. Wertheimer, Phys. Letters 18, 236 (1965).

60. M. R. Wertheimer and J. Le G. Gilchrist, preprint of paper to be published. (See Reference 59)

61. S. H. Goedemoed, C. Van Kolmeschate, J. W. Metselaar, and D. de Klerk, Physica 31, 573 (1965).

62. R. W. Rollins and J. Silcox, Phys. Letters 23, 531 (1966).

63. F. A. Otter, Jr., and P. R. Solomon, Phys. Rev. Letters 16, 681 (1966). (See also Reference 12)

64. M. R. Beasley, W. A. Fietz, R. W. Rollins, J. Silcox, and W. W. Webb, Phys. Rev. 137, A1205 (1965).

65. C. R. Wischmeyer, Phys. Letters 18, 100 (1965).